2017•2018
Faculteit Industriële ingenieurswetenschappen
master in de industriële wetenschappen: energie

Masterthesis

Evaluation and comparison of printed and microtechnically fabricated moisture sensors for textile applications

PROMOTOR :
Prof. dr. ir. Wim DEFERME

PROMOTOR :
Prof. Dr. Antoni PICARD

COPROMOTOR :
Dhr. David SCHOENFISCH

BEGELEIDER :
De heer Manoj JOSE

Matthias Booten

Scriptie ingediend tot het behalen van de graad van master in de industriële wetenschappen: energie, afstudeerrichting automatisering

Universiteit Hasselt | Campus Diepenbeek | Agoralaan Gebouw D | BE-3590 Diepenbeek
Universiteit Hasselt | Campus Hasselt | Martelarenlaan 42 | BE-3500 Hasselt

2017 • 2018

Faculteit Industriële ingenieurswetenschappen

master in de industriële wetenschappen: energie

Masterthesis

Evaluation and comparison of printed and microtechnically fabricated moisture sensors for textile applications

PROMOTOR :

Prof. dr. ir. Wim DEFERME

PROMOTOR :

Prof. Dr. Antoni PICARD

BEGELEIDER :

De heer Manoj JOSE

COPROMOTOR :

Dhr. David SCHOENFISCH

Matthias Booten

Scriptie ingediend tot het behalen van de graad van master in de industriële wetenschappen: energie, afstudeerrichting automatisering

UHASSELT

KU LEUVEN

Preface

My master's thesis traineeship in Germany was a very exciting experience from which I have learned a lot. This work is the result of a cooperation, not only between the institutions of UHasselt and the University of Applied Sciences Kaiserslautern, but also experienced Professors, PhD's and a very grateful master's student.

I would like to express my sincere gratitude to Professors Deferme Wim and Picard Antoni but also PhD's Jose Manoj and Schönfisch David for sharing their knowledge and continuous support. Further I would like to thank my parents for giving me this opportunity and all the kind people I have met during my traineeship.

Working on this thesis was both challenging and enriching. I believe it provided a wealth of knowledge and an invaluable experience which will not only help me as a future engineer but also as a person.

Matthias Booten

June 2018

Table of contents

List of tables……5
List of figures……7
List of abbreviations……9
Abstract……11
Abstract in Dutch……13

1 Introduction 15
1.1 Challenges 16
1.1.1 Different building designs 16
1.1.2 Unique characterization procedures 16
1.1.3 Moisture sensors for different application areas 16
1.2 Objectives 16
1.3 Methodology 17
1.4 Thesis preview 18
2 Sensor technology and fabrication 19
2.1 Capacitive type moisture content sensor 19
2.1.1 Introduction capacitance measuring type moisture sensors 19
2.1.2 Working principle capacitance measuring type moisture sensors 19
2.1.3 Alterations to the base design 20
2.1.4 Textile application 22
2.2 Micro technical heater type moisture content sensor 23
2.2.1 Introduction micro technical heater 23
2.2.2 Working principle microtechnical heater 23
2.2.3 Production steps 24
2.3 Printed heater type moisture content sensor 28
2.3.1 Introduction printed heaters 28
2.3.2 Production of printed heaters 28
2.3.3 Working principle 28
3 Sensor measurement setup 29
3.1 Measuring setup for capacitive type moisture content sensor 29
3.1.1 Introduction LC-100A measuring setup 29
3.1.2 LC-100A 29
3.1.3 Improving the LC100-A measuring setup 30
3.1.4 Shorter cables and the placement of the LC100-A in the climate chamber 31
3.1.5 LabVIEW Sub-VI LC-100A 32
3.2 Measuring setup for heater type moisture content sensor 34
3.2.1 Introduction 34
3.2.2 Setup components 34
3.2.3 LabVIEW program 35
4 Results 39
4.1 Results capacitive type moisture content sensors 39
4.1.1 Introduction on characterizations 39
4.1.2 Double cloth experiment 39
4.1.3 Susceptibility tests 39
4.1.4 Results of the double cloth experiment 40
4.1.5 Ramp 40-70% RH 41
4.2 Results heater type moisture content sensors 42
4.2.1 Preparation of sensor samples 42
4.2.2 Preparation printed heaters and self-regulating printed heaters 42

4.2.3 Air-water sensitivity tests and their purpose 42
4.2.4 Fundamental aspects of the air-water sensitivity test with heaters 42
4.2.5 Preparations air-water test 44
4.2.6 Calculating the amount of power for the air-water test 45
4.2.7 Results from the air-water test 47
4.2.8 Results from susceptibility tests 50
4.2.9 Results from cloth test 53
4.2.10 Results from thermal images 54
4.2.11 Heater build and performance evaluation 56
5 Conclusion and discussion 61
5.1 Measuring setups, the importance of continuous improvement 61
5.1.1 LC-100A capacitance measuring setup 61
5.1.2 Measuring setup for heater type moisture content sensors 61
5.2 Constructive improvements and alterations to the sensors 61
5.2.1 Improvements on the design of the capacitive type moisture sensors 61
5.2.2 Constructive alterations for testing with heater type moisture sensors 62
5.2.3 Conclusions of measurements 62
5.2.4 Conclusions for application of sensors 65
5.2.5 Outlook 66
Appendices 69
Bibliography 71

List of tables

Table 1 Overview of the production steps of a microtechnical heater 26
Table 2 Overview and function of used building blocks from the Sub-VI 33
Table 3 Overview and function of the program blocks in the Header Sub VI 37
Table 4 Overview and function of the program blocks of the Agilent program 38
Table 5 Overview of different heaters in varying sizes 55
Table 6 Overview of results from surface measurements 59

List of figures

Figure 1-1 Moisture content sensor of the capacitance measuring type. 15
Figure 1-2 Microheater on polyimide foil 15
Figure 1-3 Method flowchart 17
Figure 1-4 Structural overview of the chapters 18
Figure 2-1 A cross section of the base moisture content sensor [4] 19
Figure 2-2 A cross section of a resistive relative humidity sensor [5] 20
Figure 2-3 A cross-sectional view of the interdigital capacitor coated with an encapsulating protective coating and humidity responsive TiO2 layer [6] 20
Figure 2-4 Cross-sectional view of improved moisture content sensor 21
Figure 2-5 Micro-heater on polyimide foil [10] 23
Figure 2-6 Micro-heater functions of visual area [10] 23
Figure 2-7 Curing the spin coated polyimide precursor 26
Figure 2-8 Masking and lighting the image reversal resist 26
Figure 2-9 Flood lighting 26
Figure 2-10 Development of the image reversal resist 26
Figure 2-11 Evaporation of the metal and lift-off 26
Figure 2-12 Curing of the newly spin-coated polyimide precursor layer 27
Figure 2-13 Structure with the positive resist spun on the hard mask 27
Figure 2-14 Lighting and development of the positive resist 27
Figure 2-15 Structuring of the hard mask and removal of the positive resist 27
Figure 2-16 Sensor removed from support wafer 27
Figure 2-17 Printed heaters in different sizes 28
Figure 3-1 LC100-A [15] 29
Figure 3-2 Improved LC100-A measuring setup 30
Figure 3-3 Reference measurement for longer cables measurements 31
Figure 3-4 Measurement with longer cables 32
Figure 3-5 Measurement setup with shorter cables 32
Figure 3-6 Overview LC-100A Sub-VI 33
Figure 3-7 Electrical circuit [18] 34
Figure 3-8 Setup components: DAC, Power Supply, Agilent 34401A's and N-channel MOSFET 34
Figure 3-9 Overview of Agilent LabVIEW program 35
Figure 3-10 Adjustable pulse parameters 36
Figure 3-11 Contents of create header Sub VI 37
Figure 3-12 Creating and saving text files along with time and measurement data 38
Figure 4-1 Measuring setup; cloth on top of capacitive 39
Figure 4-2 Base sensor VS sensor design with encapsulation layer 40
Figure 4-3 Double cloth measurements 40
Figure 4-4 Reference measurements for the double cloth measurement 41
Figure 4-5 Ramp graph 41
Figure 4-6 Micro technical heaters in 1mm², 25mm² and 100mm² surface area respectively 42
Figure 4-7 Medium sized micro technical heater tested in air 43
Figure 4-8 Medium sized micro technical heater tested in water 44
Figure 4-9 Relative resistance changes in air and water 47
Figure 4-10 Sensitivity of a medium sensor determined from the air-water test 47
Figure 4-11 Air-water test for thick and thin small sensors 48
Figure 4-12 Sensitivity of microtechnical heaters in different sizes according to the air-water test 48
Figure 4-13 Sensitivity of a small sensor at different power levels 49
Figure 4-14 Sensitivity of printed heaters of different sizes according to the air-water test 49
Figure 4-15 Air-water test on all heaters 50
Figure 4-16 Susceptibility test of microtechnical heater S20 in air and water 51

Figure 4-17 Susceptibility test of printed heater SP8 in air and water 51
Figure 4-18 Susceptibility test of microtechnical heater S20 in water 51
Figure 4-19 Susceptibility test of printed heater SP8 in water 52
Figure 4-20 Susceptibility test of printed heater SP8 in air 52
Figure 4-21 Susceptibility test of microtechnical heater S20 in air 52
Figure 4-22 Cloth test of printed heater SP8 53
Figure 4-23 Cloth test of microtechnical heater S20 54
Figure 4-24 Temperature scale 55
Figure 4-25 Thermal image small sized micro technical heater 55
Figure 4-26 Thermal image small sized printed heater 55
Figure 4-27 Thermal image medium sized micro technical heater 55
Figure 4-28 Thermal image medium sized printed heater 55
Figure 4-29 Thermal image large sized micro technical heater 55
Figure 4-30 Thermal image large sized printed heater 55
Figure 4-31 Temperature coefficient SP7 56
Figure 4-32 Temperature coefficient S20 57
Figure 4-33 Microscope image of printed heater SP12 57
Figure 4-34 Inconsistency in thickness 57
Figure 4-35 Ink insufficiency 57
Figure 4-36 Roughness measurement printed heater SP12 line 3 58
Figure 4-37 Roughness measurement printed heater SP12 line 5 58
Figure 4-38 Printed heater SP12 vertical Dektak measurement 59
Figure 5-1 Overview of graphical results of the air-water test 62
Figure 5-2 Overview of graphical results susceptibility tests 64

List of abbreviations

General abbreviations

DAC	Digital to analog converter	*DI-water*	Deionized water
PCB	Printed Circuit Board	*RH*	Relative humidity
MOSFET	Metal-Oxide-semiconductor field-effect transistor	*DAC*	Digital Analog Converter
S	Microtechnical sensor	*SP*	Printed sensor
SS	Self-regulating sensor	*ST*	Thicker sensor

LC-100A related abbreviations

GND	Ground connection	*RX*	Read connection
TX	Transmission connection	*UART*	Universal Asynchronous Receiver Transmitter

Symbols and abbreviations from formulae

A	Surface area	C	Capacitance
c_s	Specific heat capacity	c_v	Volumetric heat capacity
C_H	Heat capacity	d	Distance capacitor plates
e	Thermal effusivity	f	Frequency
f_o	Resonance frequency	I	Current
L	Inductance	R	Resistance
S	Thickness	t	Time
T_{max}	Maximum temperature	t_{pulse}	Pulse time
U	Voltage	V	Volume
λ	Thermal conductivity	Φ	Volumetric water content
$\Delta\vartheta$	Temperature change	ε_o	Electric constant
$\frac{\Delta R}{R}$	The relative resistance change	ε_r	Relative static permittivity

Υ	Power over a certain area (Intensity)
α	Material temperature coefficient (of electrical resistance)

Abstract

Moisture sensors for textiles exist in various forms and function according to different working principles. This master's thesis is the result of a comparative research of these sensors at the University of Applied Sciences Kaiserslautern in Zweibrücken and IMO-UHasselt.

Both institutions cooperate closely but produce sensors according to different operating principles using different manufacturing technologies. At UHasselt the sensors are printed while in Zweibrücken the sensors are microtechnically fabricated. This difference formed a need to gain knowledge and put into perspective the abilities and use cases of the sensors and their production technology. Thermal moisture sensors had to be characterized using a novel thermal measurement technology initially developed for microtechnical application.

The research of this thesis takes into consideration different factors in design, production and characterization of each sensor. Alterations and improvements to both sensors and their respective measuring setups were performed and discussed. The production methods of the sensors were studied in order to gain a deeper understanding in the characteristical behavior of the different sensors.

Measurements utilizing different setups and ambient conditions are used as basis of comparison. It was noted that improvements on existing and development of new measuring setups was more beneficial for sensor characterization. The performed tests proved that sensors with thinner substrates and higher thermal coefficient were more sensitive.

The knowledge gained from this research aides in explaining the differences between the individual sensors and contributes to understanding their characteristical behavior and potential application.

Abstract in Dutch

Sensoren die het vochtgehalte meten in textielen bestaan in verschillende vormen en functioneren volgens verschillende werkingsprincipes. Deze masterproef is het resultaat van een vergelijkend onderzoek naar deze sensoren aan twee onderzoeksinstellingen, namelijk de University of Applied Sciences Kaiserslautern in Zweibrücken en IMO-UHasselt.

Beide onderzoeksinstellingen werken nauw samen op verschillende domeinen maar produceren deze sensoren volgens verschillende principes gebruik makend van verschillende productie technologieën. Op IMO-UHasselt worden de sensoren geprint terwijl de sensoren op de University of Applied Sciences op micro technische wijze worden gefabriceerd. Uit dit verschil ontstond de nood aan het vergaren van kennis en het in perspectief stellen van de capaciteiten en toepassingsgebieden van zowel de sensoren als de technologie waarmee ze gefabriceerd worden. Verder moesten thermische vocht sensoren gekarakteriseerd worden door middel van een nieuwe meettechnologie die voorheen enkel voor micro technische toepassingen bestemd was.

De masterproef houdt rekening met de verschillende factoren in ontwerp, productie en karakterisatie van elke sensor. Aanpassingen en verbeteringen aan zowel sensoren als hun bijhorende meetopstellingen werden uitgevoerd en besproken. De productie methoden werden bestudeerd teneinde een diepgaand begrip te vormen van de karakteristieke gedragingen van de sensoren.

Verder vormen metingen die gebruik maken van uiteenlopende opstellingen en omgevingstoestanden de basis van het vergelijkend onderzoek. De tests bewezen dat de sensoren met dunnere substraten en hogere thermische coëfficiënt gevoeliger waren.

De vergaarde kennis draagt bij in het verduidelijken van de verschillen tussen individuele sensoren hetgeen contribueert in het begrijpen van hun karakteristieke gedrag en potentiële applicatie.

1 Introduction

This master's thesis centers around moisture sensors on textiles and took place at the University of Applied Sciences Kaiserslautern in Zweibrücken. The majority of the work was conducted in the Department of Micro Systems Technology. This department specializes on sensors for smart textiles among other micro technical applications [1]. The University of Applied Sciences cooperates closely with IMO-UHasselt in various domains. The thesis combines the expertise of both institutions to form a broader and more qualitative research in the field of moisture sensors on textiles. The micro technical expertise of the University of Applied Sciences and the printed electronics expertise of IMO-UHasselt complement each other in this work [2].

During a preparatory period a moisture content sensor of the capacitance measuring type was produced and characterized at IMO-UHasselt. Similarly in Zweibrücken a micro-heater on polyimide foil was already developed for sensor application. The methods of production between IMO UHasselt and the University of Applied Sciences in Zweibrücken differ because they respectively use printed-and microtechnical methods which leads to different sensors for similar application areas. The two produced sensors along with possible alterations on their design and other types of sensors for moisture measurement are compared within the master thesis. In the figures below a capacitive type sensor from IMO-UHasselt can be seen in Figure 1-1 while in Figure 1-2 a microtechnical heater produced in Zweibrücken can be seen.

The research is done in such a manner that not only the differences in their characteristics or design is understood but also a knowledge bridge between the two institutions is formed.

Figure 1-1 Moisture content sensor of the capacitance measuring type.

Figure 1-2 Microheater on polyimide foil

1.1 Challenges

Both IMO UHasselt and the University of Applied Sciences Zweibrücken work on moisture sensors. However, their means and methods are quite different, resulting in different sensor types. From these differences a need was established to gain knowledge of the sensors, the production methods and their possible applications. Two different measuring setups were used which the student had to alter or improve in such a way that they could be used for comparison of the sensors of both institutions. Thereafter, various tests were performed in order to do comparative research on all types.

1.1.1 Different building designs

To understand the implications of building these sensors in different ways and the difference in their respective performance a characterization of all sensors was performed. There was a need to make sure that the characterization of both sensors was comparable and to make sure both climate room setups and programs overcame these difficulties.

1.1.2 Unique characterization procedures

As important as a qualitative design or sensor build may sound, without proper characterization knowledge the sensor will become hard to utilize for the intended application areas. Therefore in order to properly utilize and compare different types of sensors efficient characterization was required. The characterization needed to take into account the different aspects of the sensors such as the fact that they possibly had to be brought in contact with the textile which was desired to be measured or were already printed upon a textile substrate.

1.1.3 Moisture sensors for different application areas

The moisture sensors developed for IMO-UHasselt were for instance intended for use in the medical sector, more specifically wound monitoring. These sensors had to be able to measure the presence of wound fluids. At the University of Applied Sciences Zweibrücken research was done in order to properly characterize moisture in apparel. Although the intended application domain of the sensors was different, comparative research was needed which also took into account the requirements of their end applications.

1.2 Objectives

To suit the main objective of comparison between moisture sensors, different types of printed and micro technical sensors are also compared to each other. To this end the research must be quantitative in terms of collecting factual measurement data from sensor characterizations in order to form proper understanding of the characteristic behavior of the sensors. It must also be qualitative in terms of interpreting the measurement results and correctly forming the base explanation which relates the differences in design, method of production, method of sensing and type of sensor to physical phenomena which result in those measurement results.

To the end of realizing both qualitative and quantitative research, literature study and field testing of sensor (characterization or building) applications was needed to gain knowledge. This naturally meant that the master's thesis needed to result in improvement of knowledge for the student and all parties involved. Improvements of knowledge on these sensors, their design, production, characterization, and of course area of application was aimed to be supportive for current and future use cases.

Possible influence from ambient conditions such as temperature, relative humidity, contact to certain materials on sensor measurements needed to be researched so improvements and use cases could be respectively realized and defined.

1.3 Methodology

To achieve the objectives mentioned in the former paragraph, knowledge of the fabrication and working principle of all used sensors needed to be obtained. Gaining knowledge of the fabrication principle was be done via literature study and producing or participating in the production of the sensors. The working principle of the sensors was also to be learned from literature study and by studying information gained internally in the institutions were the thesis took place. Since comparison is key in this thesis, tests had to be performed on the sensors. A general overview of the utilized approach can be found in the flowchart in Figure 1-3. Following tests were planned as part of the general approach devised to compare the sensors:

- Both the capacitance type sensor as well as the thermal type sensor were tested in a climate chamber under various temperatures and relative humidities.
- The printed and micro technical heaters were tested in surroundings of both air and water.
    - The capacitive type sensor was measured by a LC-100A measuring device.
    - The thermal sensors was measured by an Agilent 34401A in combination with an electronic switching circuit.
- There were general combined tests of the thermal type and the capacitance type sensor at the same time.
- The linearity of both thermal and capacitive type was tested using the gravimetric method. This method implies drying textiles on a scale in order to measure and evaluate linearity in measurement results for evaporating moisture.
- The moisture sensors were tested with various textiles (for instance cotton vs polyester or different clothing pieces t-shirt, socks,…).
- Comparative tests of printed and lithographical thermal moisture sensor included but were not limited to:
    - analysis of resistance dependence on temperature (for instance in an oven);
    - evaluation of linearity of collected measurement data;
    - observe heated sensors under thermal-camera to monitor if they show hotspots ;
    - measurements in dry environments and humid environments ;
    - testing sensors with wet textiles to monitor for linear values by measuring textile water content in relation to the measured value.

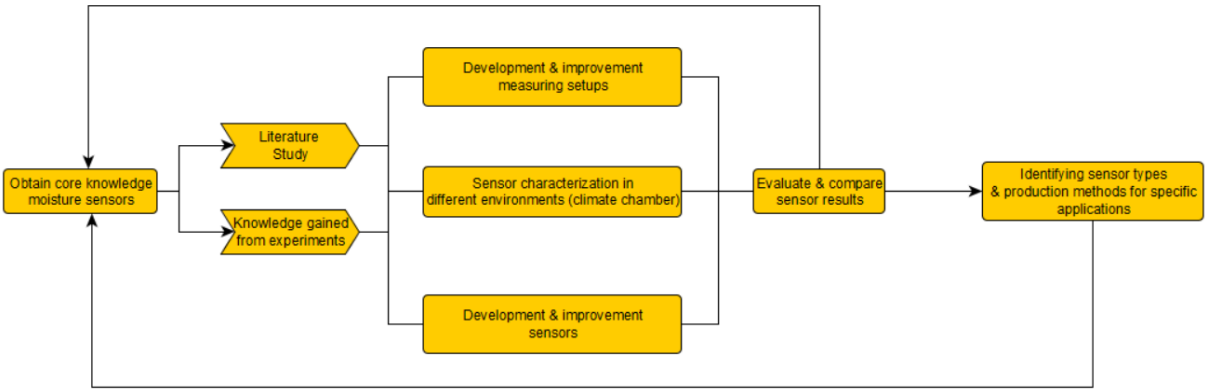

Figure 1-3 Method flowchart

1.4 Thesis preview

Figure 1-4 gives a structural overview of the chapters of which this thesis consists.

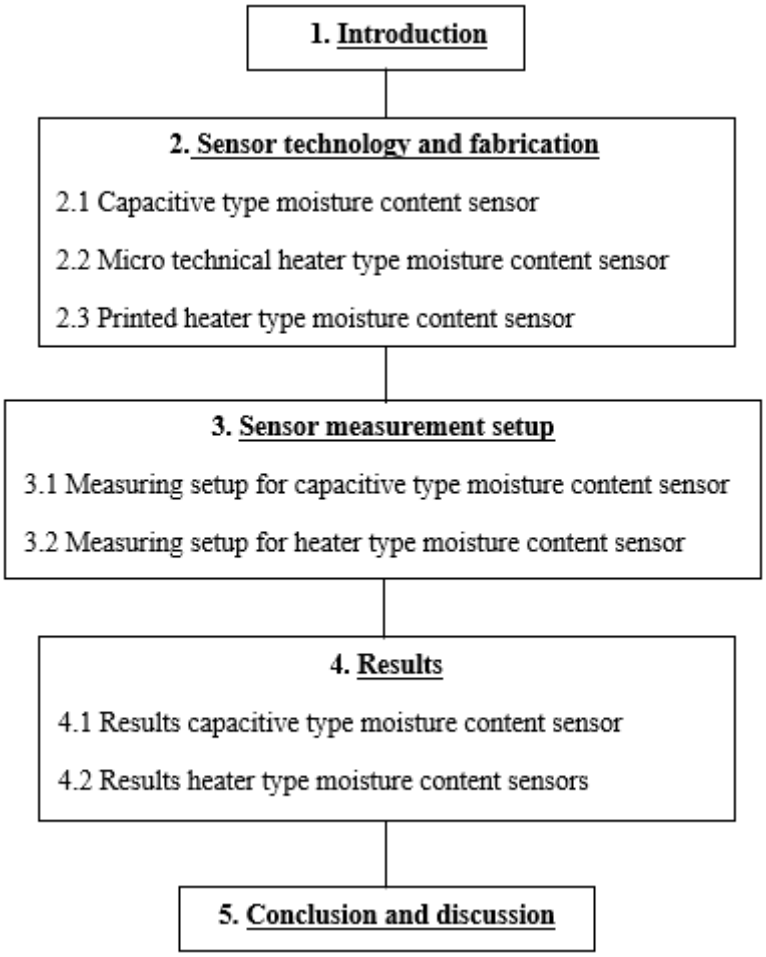

Figure 1-4 Structural overview of the chapters

This thesis is constructed around 3 pillars that form the foundation for understanding and comparing all sensors. First, the different types of moisture content sensors will be explained in chapters 2,3 and 4. Chapter 2 will involve capacitive type sensors while chapters 3 and 4 will shed light on micro technical and printed heater type sensors respectively. The next pillar involves the measuring setups for the capacitive and thermal type sensors which are included in chapters 5 and 6. Finally, the measurement results of these sensors can be found in chapters 7 and 8. These main pillars will act as the material used for the comparison of sensors and the base for the conclusions drawn in chapter 9.

2 Sensor technology and fabrication

2.1 Capacitive type moisture content sensor

2.1.1 Introduction capacitance measuring type moisture sensors

A literature study was performed intended to gain knowledge on different types of moisture sensors and to select a suitable sensor to be printed. The sensor was intended for wound monitoring and as a result of this, it needed to be a moisture content sensor. The literature study resulted in a printable moisture content sensor of the capacitive type being chosen. Factors such as the ease of printability, measurability and the possibility to produce a linear output signal directly in relation to moisture content levels played an important part in making this decision.

2.1.2 Working principle capacitance measuring type moisture sensors

The basic principle of the chosen sensor is quite simple, there is a substrate which is exposed to moisture and experiences a resulting change in conductivity. Therefore a dielectric layer between conductive ink and the interdigitated structure is needed. This dielectric layer acts as an insulator to prevent shortcuts. The concept behind this sensor is the measuring of the capacitance between the conductive lines of the interdigitated structure. The measured value of the capacity depends on the capacity between conductive lines, the capacitance through the surrounding air and the capacitance through the substrate. By shortening the distance of the line spacing of the electrodes and increasing their conductivity the sensors can become more sensitive [4].

The sensor setup can be seen as 3 capacitors in parallel. The total capacitance is the sum of the earlier mentioned individual capacitances and can be found in equation 2.1. The chosen base design for a capacitive type moisture content sensor can be seen in Figure 2-1 [4].

$$C_v = C_1 + C_2 + \cdots + C_n \qquad (2.1)$$

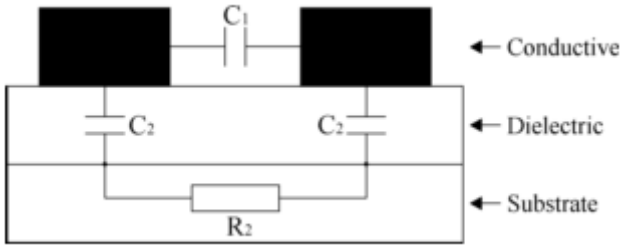

Figure 2-1 A cross section of the base moisture content sensor [4]

If the moisture content of a cellulose-based substrate is changed, its resistance is also changed and this will lead in to a change in capacitance through the substrate [4]. This is due to the permittivity of the dielectric medium changing which is explained in greater detail in paragraph 2.1.3. By measuring the capacitance in the sensor the moisture content of the cellulose based substrate can be monitored.

2.1.3 Alterations to the base design

A possible problem found early in the original design was the possibility of an internal relative humidity sensor. The conductive layer of the interdigit structure and the dielectric layer upon which it was printed form a resistive relative humidity sensor, as can be seen in Figure 2-2 [5].

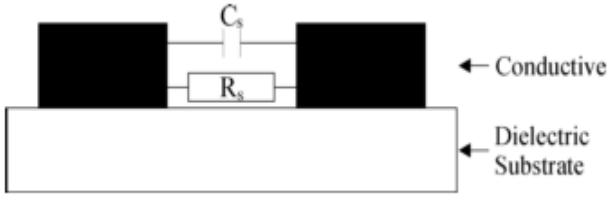

Figure 2-2 A cross section of a resistive relative humidity sensor [5]

However, the intended sensor is a moisture content sensor. It is preferred that the sensor isn't susceptible to any ambient conditions such as relative humidity changes and strictly measures the moisture content of the textile substrate. To achieve this an encapsulating TiO_2 layer was applied over the conductive interdigit structures as seen in Figure *2-3*[6]. This had as goal encapsulating the layers which formed a resistive relative humidity sensor in order to reduce the influence of ambient humidity. The idea of the added layer was found in the application of LC-resonant circuit sensors. In the case of LC-resonant circuit sensors the TiO_2 encapsulating layer is used both as a humidity responsive and protective layer as displayed in Figure *2-3* [6]. The TiO_2 layer has a relative permittivity of 3.8 while the relative permittivity of water and air being 81 and 1 respectively[6] [7]. This meant the encapsulating layer functioned as a dielectric that would not interfere with the capacitance between the interdigit structure while shielding it from direct contact with air to lessen the potential interference of the internal resistive relative humidity sensor. The effective permittivity of water is higher than that of TiO_2which leads to the increase of the effective permeability of the TiO_2 coating which means the electrical permittivity will change accordingly in response to humidity. This will lead to a lower resonant frequency of the sensor [6].

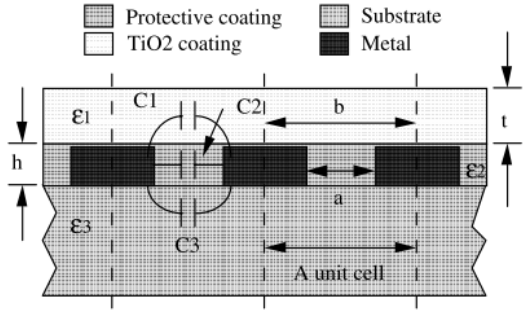

Figure 2-3 A cross-sectional view of the interdigital capacitor coated with an encapsulating protective coating and humidity responsive TiO_2 layer [6]

The effect of self-resonance frequency is described as the frequency at which resonance occur due to the capacitor's own capacitance and residual inductance [8]. Further it is known as the frequency at which the impedance of the capacitor becomes zero. This leads to the formulae found below. From equation 2.2 , equation 2.3 is determined.

$$j2\pi fL + \frac{1}{j2\pi f_o.C} = 0 \tag{2.2}$$

$$f_o = \frac{1}{2\pi\sqrt{LC}} \tag{2.3}$$

This indicates that when the resonant frequency lowers the capacitance increases. Which proves that the added T_iO_2 layer preserves the characteristic trait of the capacitive type moisture content sensor to have an increasing output signal directly proportional to the measured moisture in the sensor. Figure *2-4* gives a full overview of the resulting design that was chosen.

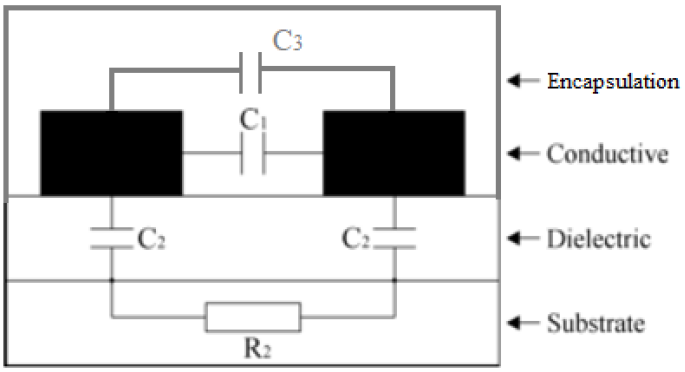

Figure 2-4 Cross-sectional view of improved moisture content sensor

2.1.4 Textile application

It is generally known that cellulose-based papers lose strength when exposed to high levels of humidity [4].Therefore one should look into the different possibilities with textiles. When evaluating textiles for use in moisture sensors certain attributes such as wettability but also the "impregnation area" should be considered. The wettability is defined as the time in seconds for a drop of water to sink into the fabric. The impregnation area is the area where the water impregnates the textile, the larger the area the faster and more clear the detection of the moisture can take place [9]. Thus a textile with large impregnation area and good wettability is both fast acting and more decisive because of a larger measuring area. Wider impregnation areas allow for use of the sensors in a wider monitoring area. A test done by Parkova en Ziemele [9] showed the differences in different textiles in terms of wettability and wet area. The test showed that Polyester was the fastest absorbing material but a textile made out of 50% Polyester and 50% Cotton combined this fast absorption with a large impregnation area. This is to be considered as a testing material.

Textiles are however, a very different material to print on then paper. One of the important factors is the fact that the silver ink used for printing will sink into the textiles. This may result that the spacing between conductive lines of an interdigitated structure becomes smaller than anticipated. One needs to bear this in mind to avoid illogical printed structures or worse a printed structure which short circuits in the case of touching electrodes. Another attribute of textiles can be called the wicking of the fluid. This can be related to moisture transport. The wicking increases by rising viscosity of the fluid and decreases with increase in the surface tension of the liquid, capillary radius and contact angle [9]. In the end, a textile of 100% polyester was chosen due to its fast absorption and evaporation times which added to the usability of the sensor. The fact that 100% polyester was relatively easy to print upon was also considered an added benefit.

2.2 Micro technical heater type moisture content sensor

2.2.1 Introduction micro technical heater

The micro-heaters produced in the cleanroom of the University of Applied Sciences Zweibrücken are developed on polyimide foil for sensor application. The sensor application is measurement of moisture content in textiles utilizing the thermal based moisture measurement principle further discussed in paragraph 2.2.2. The sensor is visually introduced in the pictures below. Figure *2-5* depicts a produced heater on a PCB ready to connect to measuring devices [10]. The functions of the visual areas are introduced in Figure 2-6. The heater is produced with 4-wire connector to be able to make 4-wire resistance measurements which are more accurate than normal two wire measurements.

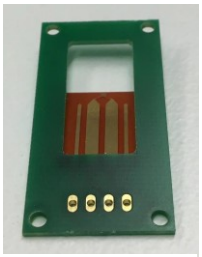

Figure 2-5 Micro-heater on polyimide foil [10]

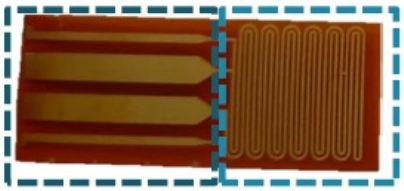

Figure 2-6 Micro-heater functions of visual area [10]

2.2.2 Working principle microtechnical heater

A heater is placed in contact with a textile with a certain amount of moisture in it. When the heater is turned on, heat will be transported to the textile. This heat transport depends on the moisture content of the textile due to its heat capacity and thermal conductivity. Due to heating the sensor's temperature shall increase in function of the volumetric heat capacity and thermal conductivity. The temperature increase of the sensor is also in function of the thermal effusivity, which can be found by calculating the square root of the product of the Volumetric heat capacity and the thermal conductivity as seen in equation 2.5 [10]. This function correlates to the function of the water content which allows the amount of moisture in the cloth to be determined as seen in equation 2.4. The overview of microtechnical heaters can be found in Appendix 1.

$$\Delta\vartheta = f(C_v, \lambda) = f(e) \cong f(\Phi) \tag{2.4}$$

$$e = \sqrt{\lambda . C_v} \tag{2.5}$$

The sensor resistance shall change accordingly to its temperature change. The relative resistance change is linked to the product of change in temperature of the material and the material's temperature coefficient of electrical resistance [10].

$$\frac{\Delta R}{R} = \Delta\vartheta . \alpha \tag{2.6}$$

The goal then of measuring with heaters is measuring the change of resistance and using it to determine the temperature change. Since the temperature change is in function of the thermal effusivity which can be linked to the volumetric material water content, the moisture content in the cloth can be determined.

2.2.3 Production steps

The following production steps are part of the most recent production process-flow as mentioned in [11]. The illustrations that were made for the purpose of explaining the manufacturing steps were based on information gained from participating in part of the production of these heaters and can be found in Table 1. This process-flow consists of the following steps:

- Substrate preparation
- Producing a polyimide layer
- Production of the heater structures
- Production of polyimide passivated contact holes
- Removal of the sacrificial layer

Substrate preparation

To add strength during the production process the heaters are be built upon a support wafer. Once they are finished, those newly produced heaters will be removed from the wafer by means of etching the sacrificial layer of the support wafer.

Producing a polyimide layer

By means of spin-coating a homogeneous layer is produced from polyimide precursor upon the sacrificial layer. Afterwards the solvents are removed by means of a soft bake. To transform the polyimide precursor into the polyimide a temperature curing is done. Figure *2-7* shows the structures before and after curing during which water separates which turns the polyimide precursor in polyimide.

Production of the heater structures

During the next steps a layer of image reversal resist is spin-coated on. To get rid of the solvents this is again followed by a soft bake. Following the soft bake, the resist has to cool down and rehydrate. Using a mask aligner, the mask structure gets transferred over in the resist. The part visualized in Figure *2-8* upon which the (UV)-light shines becomes soluble. This means the lighted solvent sections of the resist interconnect which makes it possible to produce the needed undercut by doing an image reversal bake.

Following this step the resist has to cool down and rehydrate again in order to separate those interconnected sectors from the rest. The sectors that are still being photoactive will be loosened up by flood exposure (UV-light) as seen in Figure *2-9*. After this flood exposure the development can be done.

This development is achieved by means of an alkaline developer. After a predetermined development time, the reaction has to be stopped which is done by rinsing the entire wafer with DI-water followed by a drying of the wafer. Figure *2-10* shows the structure after development of the resist.

Vapor deposition is used for adding the next layer consisting of a suitable metallization. The resist layer needs to be removed in order to expose the heater structures. To achieve this, the wafer is placed in a suitable solvent such as Acetone. Figure *2-11* visualizes the result of the Acetone dissolving the resist revealing the heater structures. Remaining metal particles are removed by rinsing the wafer in DI-water. Afterwards the wafer is dried.

Production of the Polyimide passivate contact areas

To shield the metallic heater structures from ambient influences such as for instance humidity which might cause short circuits, dielectric passivation layers have to be applied (on the surface). By means of spin coating another Polyimide precursor layer will be applied on top. Directly

after which a soft bake shall follow to drive out the solvents. In order to transform the precursor into solid Polyimide the passivation layer has to be cured as displayed in Figure *2-12*.

It is for example suitable to bring structure to the polyimide passivation by means of a dry etching process. Therefore the next step consists of putting on a hard mask on the polyimide layer by means of vapor deposition. This hard mask can tolerate physical and chemical influences while etching. Figure *2-13* shows the positive resist spun on the hard mask. After another soft bake the solvents are driven out upon which the resist layer has to cool down and rehydrate again.

The mask structures of a second mask get transferred by UV-light by means of a mask aligner. In the second mask, all the sectors of the contact pads will become alkaline solvable. The solvable sectors will be dissolved in the alkaline developer after which the wafers will be rinsed in Di-ionized water again after which they are dried. The resulting lacquer mask serves for structuring the hard mask. These processes can be seen on Figure *2-14*.

The hard mask is opened my means of wet chemical etching. After the structuring of the hard mask the resist layer can be removed by means of Acetone. The result of these processes can be seen on Figure *2-15*. The following step is rinsing the wafer in Isopropanol and di-ionized water and drying.

The sectors on the hard mask which are now opened can now be etched. The opening of the contact pads happens afterwards of the polyimide can be done. This opening of the contact pads is done by means of dry-etching. The hard mask is then removed by means of wet chemical etching.

Removal of the sacrificial layer

The finished heater elements can now be removed from the support wafer. This can be achieved by wet chemically etching the sacrificial layer. Figure *2-16* shows the separated heater and support wafer. The end result is a heater which has a metal layer with a thickness of 300nm and two polyimide layers of 10µm each.

Overview of production

Table 1 Overview of the production steps of a microtechnical heater

Production step	Legend
Curing polyimide precursor 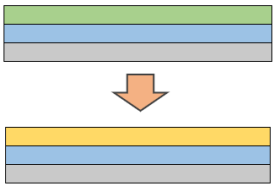 Figure 2-7 Curing the spin coated polyimide precursor	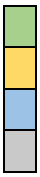 Polyimide precursor Polyimide layer Sacrificial layer Support wafer
UV-lighting 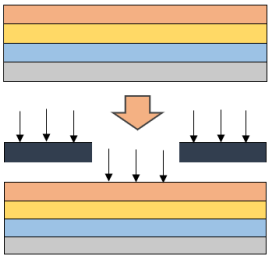 Figure 2-8 Masking and lighting the image reversal resist	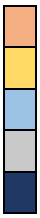 Image reversal resist Polyimide layer Sacrificial layer Support wafer Cover from light
Image reversal bake Positive resist turns negative as needed for undercut that allows spacing between metal.	
Flood exposure 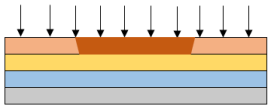 Figure 2-9 Flood lighting	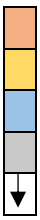 Image reversal resist Polyimide layer Sacrificial layer Support wafer UV-light
Development of the image reversal resist 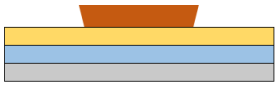 Figure 2-10 Development of the image reversal resist	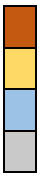 Developed resist Polyimide layer Sacrificial layer Support wafer
Evaporation of the metal and lift-off 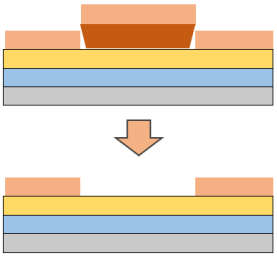 Figure 2-11 Evaporation of the metal and lift-off	 Metal Polyimide layer Sacrificial layer Support wafer

Curing

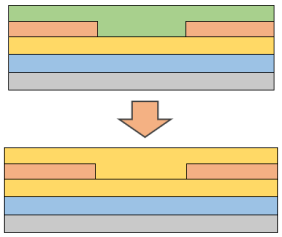

Figure 2-12 Curing of the newly spin-coated polyimide precursor layer

Polyimide precursor
Metal
Polyimide layer
Sacrificial layer
Support wafer

Spin coating of the positive resist

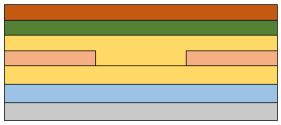

Figure 2-13 Structure with the positive resist spun on the hard mask

Positive resist
Hard mask
Metal
Polyimide layer
Sacrificial layer
Support wafer

Lighting and development

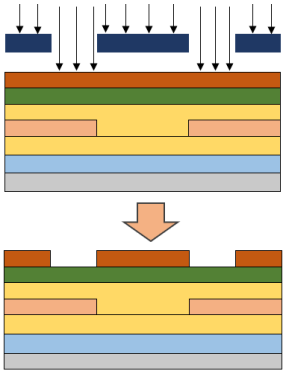

Figure 2-14 Lighting and development of the positive resist

Positive resist
Hard mask
Metal
Polyimide layer
Sacrificial layer
Support wafer
UV-light
Cover from light

Wet chemical etching and resist removal

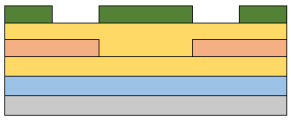

Figure 2-15 Structuring of the hard mask and removal of the positive resist

Hard mask
Metal
Polyimide layer
Sacrificial layer
Support wafer

Separation of heater from support wafer

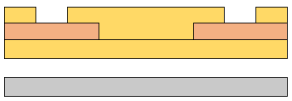

Figure 2-16 Sensor removed from support wafer

Metal
Polyimide layer
Support wafer

2.3 Printed heater type moisture content sensor

2.3.1 Introduction printed heaters

The printers function in the same manner as the microtechnical heaters as described in chapter 2.2.2. The self-regulating heaters alter their resistance in accordance to their temperature thereby behaving as both a positive- and negative temperature coefficient as seen in Appendix 3. To prevent a resistance corresponding with two temperatures and thereby two measurement values, the self-regulating heater was tested only in the area of positive temperature coefficient under 70°C.

2.3.2 Production of printed heaters

The printed heaters are all produced on polyimide foil substrates of 50 and 75µm thick, which were the thinnest foils available at time of production. Conductive lines were printed using silver ink in a screen printing process and encapsulated using a layer of polyimide tape of 50µm thickness [12]. In the cases of self-regulating heaters a carbon coating 4 to 6µm was applied before the conductive lines were printed. A printed equivalent of the microtechnical heater was built by IMO-UHasselt. These heaters can be seen in Figure *2-17* below. In this figure the round shaped heaters are the regular printed heaters while the black carbon coated self-regulating heater has a rectangular shape. The overview of printed heaters and their properties can be found in Appendix 1.

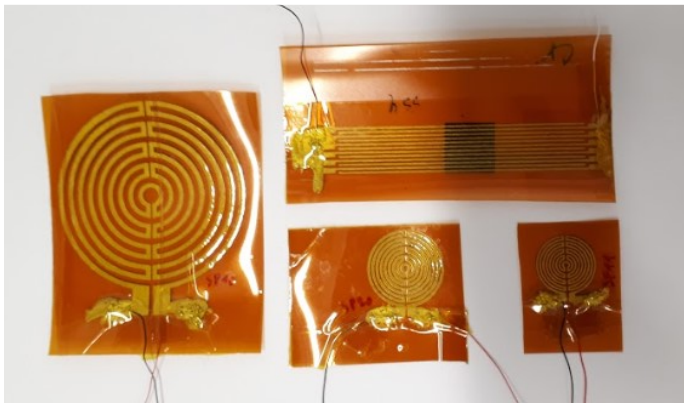

Figure 2-17 Printed heaters in different sizes

2.3.3 Working principle

The working principle of all printed heaters is the same that is mentioned in paragraph 2.2.2 where the working principle of the micro technical heater is explained. This is due to the normal printed and printed self-regulating heaters are positive temperature coefficient materials. It should be mentioned that the self-regulating heater will only be usable for these kinds of measurements up to a certain temperature. After this temperature point of around 70° is reached, the properties of the heater will see to it self-regulating its resistance according to temperature. This means that the self-regulating heater is not suited for measurements over a certain temperature. This is due to the fact that a single resistance would otherwise coincide with two temperature values. A chart of these working behaviors of the self-regulating heaters can be found in Appendix 1.

3 Sensor measurement setup

3.1 Measuring setup for capacitive type moisture content sensor

3.1.1 Introduction LC-100A measuring setup

The measuring setup consists of three important modules: the LC100-A measuring device, the sensor attachment platform and of course the sensor itself. The LC100-A was altered so continuous readouts were possible via LabVIEW. This was done by attaching 3 cables to the TX (transmission), RX (read) and GND (ground) connecting them with an ARDUINO® USB-shield. This makes it possible to read out the UART signal from the LC-100A.

3.1.2 LC-100A

The LC 100-A is a pre-programmed microcontroller which is able to measure inductivity L [H] as well as capacity C [pF]. The meter is based on the LC resonant principle [13].This device was chosen for capacitance measurements because it showed superior accuracy and measuring capabilities when measuring capacitance in the picofarad range. This superiority means it has a large capacitance measuring range starting from 0.01pF reaching all the way up to 100mF with accuracy of at least 5% [14]. In Figure *3-1*, the LC100-A can be seen along with a layout of its various controls [15].

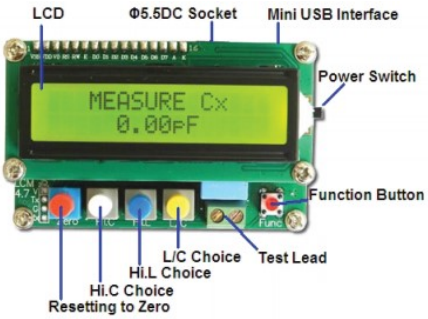

Figure 3-1 LC100-A [15]

3.1.3 Improving the LC100-A measuring setup

At first a setup was used using long cables which were connected to the sensors via magnets so they would not damage the printed layers. Because of the longer climate chamber and the greater amount of sensors which had to be tested a setup was used which needed longer cables.

When testing was performed in Germany the setup was altered. A platform was designed where the sensors would be placed upon. The platform consists of copper tape attached on top of the platform to make contact with the sensors. The parts of the copper tape that shouldn't make contact with the sensors are covered with electrical tape under which the connection wires for the LC-100A were soldered.

This entire setup is now placed within the climate chamber. This proved for more consistent results due to lesser interference from longer cables. The biggest benefit is that the new setup makes it easier to compare with thermal sensors. This is because the sensors are placed on a platform with electrical contacts so the sensing substrate of the sensor points upwards and away from the platform. This platform can be seen in Figure *3-2*.

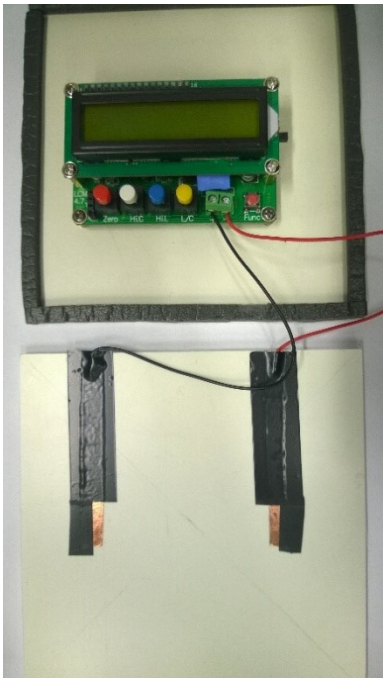

Figure 3-2 Improved LC100-A measuring setup

3.1.4 Shorter cables and the placement of the LC100-A in the climate chamber

As mentioned earlier the measurements with the longer cables showed less consistency. Longer cables have an increased resistance and are also more susceptible to noise. Noise is created within test leads when they are in the influence of a magnetic field which is changing or if the leads are moving within that field, for this reason, leads should be kept as short as possible and shouldn't be moved during measurement [16].

In the following graph shown in Figure *3-3* the basic form of the climate chamber program and actual measurements from reference sensors is displayed. The used sensor is an Sensirion SHT31 which has the following accuracy 2 %RH and ± 0.2 °C [17].

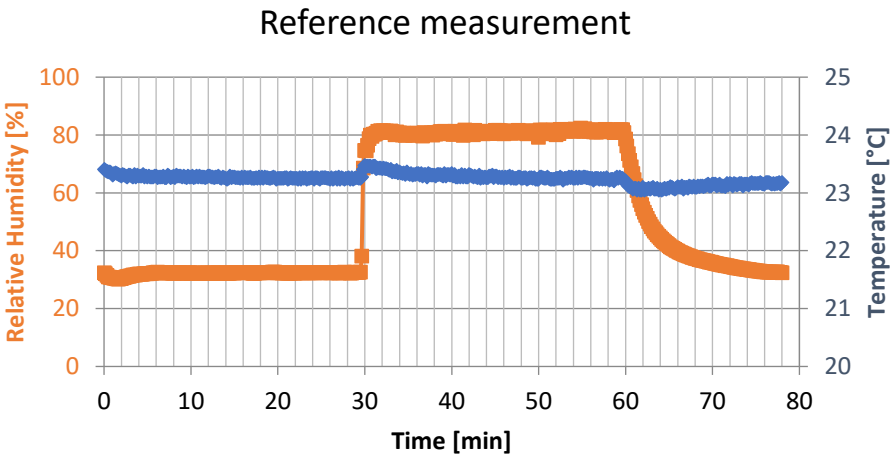

Figure 3-3 Reference measurement for longer cables measurements

During the first hour the Relative Humidity [%] is kept at a constant value of around 30%. This period is followed by a steep step from 30 to 80% relative humidity in under a minute after which the new level of humidity is maintained for another 30 minutes. The last 20 minutes the program drops back to the original value of 30% relative humidity. During the course of the whole program cycle the temperature is programmed to stay constant at 23°C.

In the following graphs the results for the same program with measurements done with longer cables (Figure *3-4*) as well as shorter cables (Figure 3-5) are displayed. The moisture will soak into the textile but the absorption will slow down overtime due to the textile getting saturated. From comparison of both graphs it quickly becomes apparent that the long cables which have a higher resistance and receive too much noise lead to the real signal being muted.

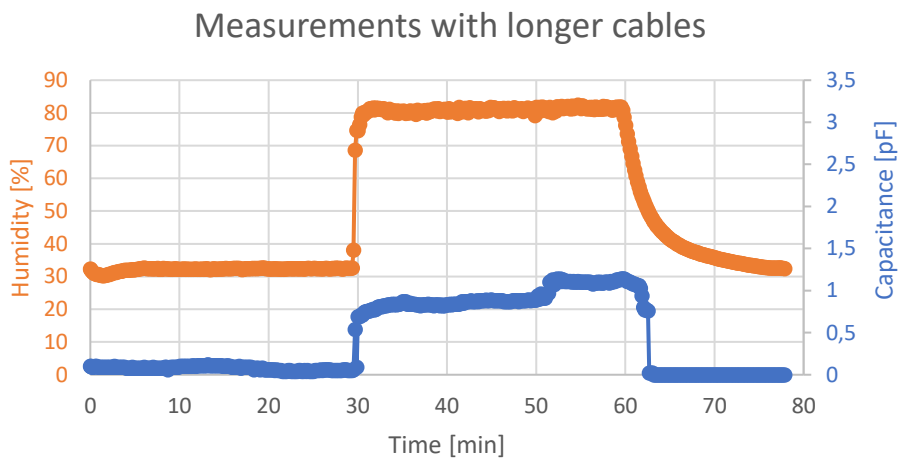

Figure 3-4 Measurement with longer cables

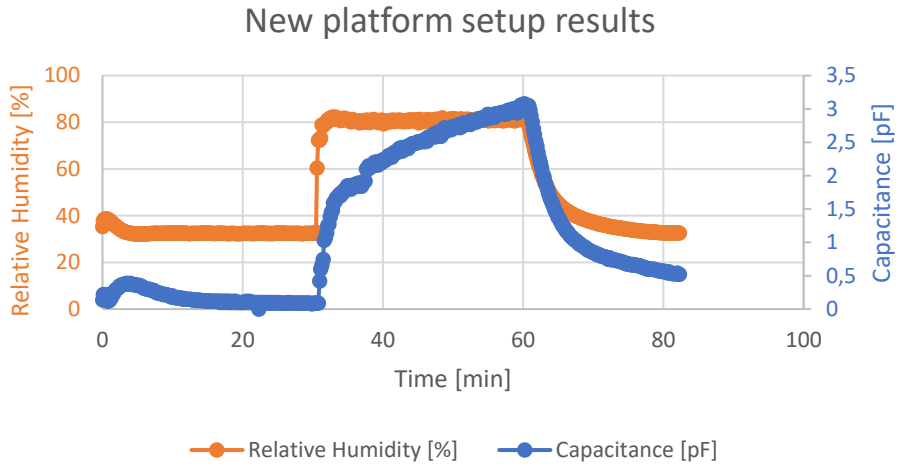

Figure 3-5 Measurement setup with shorter cables

3.1.5 LabVIEW Sub-VI LC-100A

The LC-100A is able to communicate with external software if a connection is made with the RX and TX port of the device. In order to do this the GND is also connected to achieve a common ground for measurements. The LC-100A Sub-VI is used within a program which is already able to read in values from a scale and a reference moisture sensor. By adding this Sub-VI, the former LabVIEW program is able to read out capacitance measurements as well. The LC-100A sends out the measurement values in a reverse order. The added Sub-VI reorders these numbers again so a correct readout can be performed.

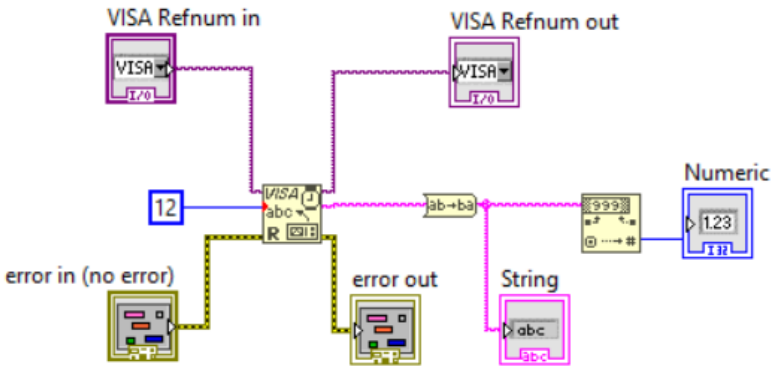

Figure 3-6 Overview LC-100A Sub-VI

Table 2 Overview and function of used building blocks from the Sub-VI

Program block	Function	Program block	Function
VISA Refnum in	Provides the I/O data of the measurement device	VISA Refnum out	Reads out the I/O data of the measurement device.
error in (no error)	Used to read in and define error data.	error out	Reads out any error data.
	Reads the number of bytes specified by visa resource name and turns the data in a read buffer.		Reverses the order of data within the string that passes this block.
	Converts the decimal string to a number.	Numeric	Defines the read-out data as the numeric long integer type.
	The amount of Bytes that the program reads from a single measurement.		

3.2 Measuring setup for heater type moisture content sensor

3.2.1 Introduction

In order to work with the heater and use it for measuring purposes it must be powered by a DC-power supply. A DC pulse is needed for 300ms. This is achieved by using an n-channel MOSFET which is controlled by means of a signal on its gate. The signal is provided from the analog output from an NI myDAQ mx device which is controlled by a LabVIEW program. The current is measured by an Agilent 34401A multimeter which is connected to a computer via RS-232 cable made for asynchronous serial communication. The current is then stored by the LabVIEW program as a text-file. This current can later be recalculated to the electrical resistance which can be used to estimate the amount of moisture. This circuit is shown below in Figure *3-7* [18].

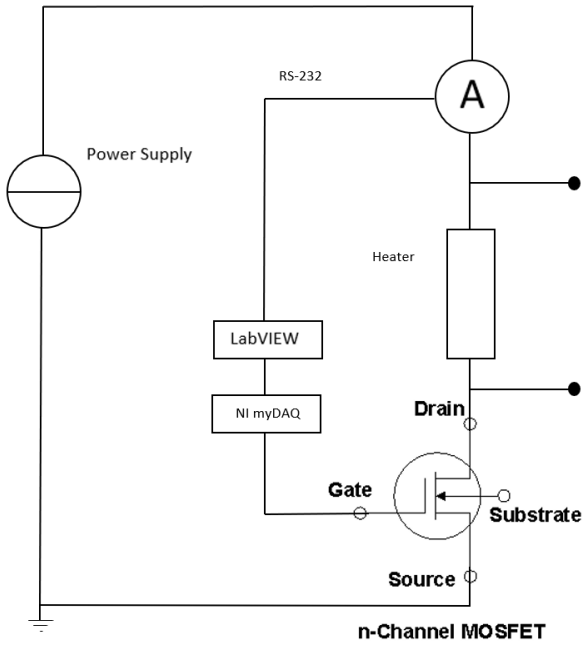

Figure 3-7 Electrical circuit [18]

3.2.2 Setup components

The various components of which the purpose was explained in paragraph 3.2.1 are displayed below. From left to right, following components are displayed: myDAQ DAC, Power Supply, Agilent 34401A and the N-channel Mosfet.

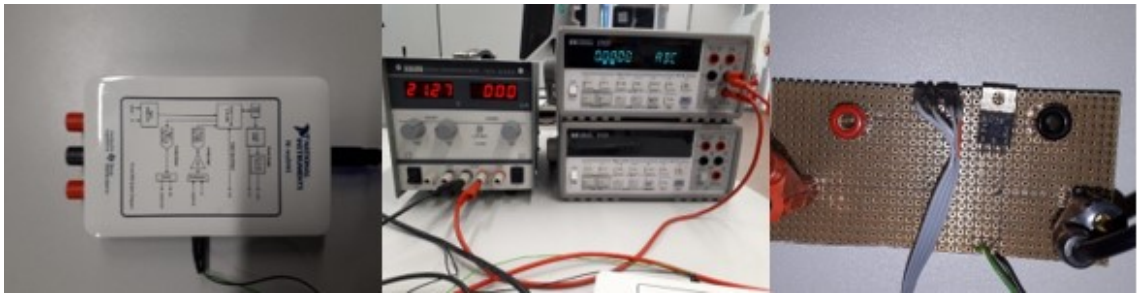

Figure 3-8 Setup components: DAC, Power Supply, Agilent 34401A's and N-channel MOSFET

3.2.3 LabVIEW program

A Labview program was made for measurements with the Agilent and the circuit displayed in Figure *3-7*. This program utilized excisting Sub VI's in combination with newly added elements.

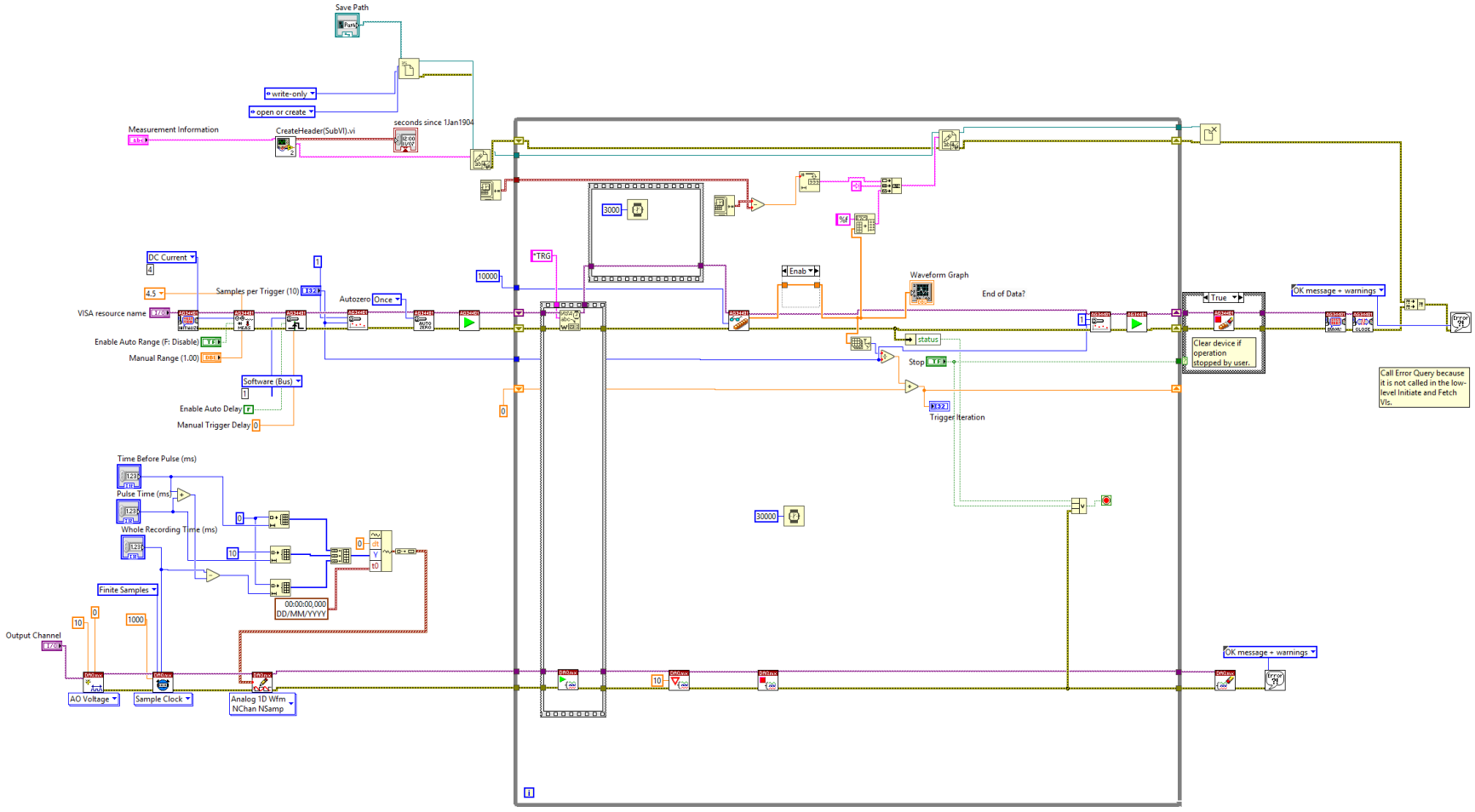

Figure 3-9 Overview of Agilent LabVIEW program

LabVIEW program

The LabVIEW program is based on the general straight forward structure that is standard to LabVIEW. This means the graphical code is executed from the left to the right. Unlike other architectures such as the state machine which is also often used for measuring programmes, this program does not change its state depending on output from the previous state. Rather, the input signals determine the continuous state of the program in general. The program consists of Sub-Vi's specific to the Agilent 34401A which control certain functions such as triggering and sensitivity of a unit. Sensitivity can for instance be seen as measuring in Ampére or milli Ampéres. Other functions had to be conceived by adding new code. The new code needed to be able to adjust pulse parameters for the MOSFET in the electrical circuit of the measuring setup, start measurements simultaneous to sending out control pulses for the MOSFET, make a measurement files with appropriate headers and include measurements with their respective time of measuring.

Adjustable pulse parameters

In order to achieve continuously identical measurements the parameters regarding the measurement pulses had to be adjustable for different measurements. These adjusted parameters are connected to the Timing Configuration (sample clock) and the Write Waveform Sub VI's in order to function properly with the internal software of the Agilent multimeter. Figure *3-10* displays the code which is used to adjust the time before the pulse, the pulse time itself and the whole recording time. During the time before the pulse, the MOSFET is open because it receives 0 Volt. During the pulse time, the MOSFET receives 10V and closes the electrical circuit. Finally during the time after the pulse the MOSFET will receive 0 Volt again leading the MOSFET to stay open. These three times together form the total controlling time cycle which control the DAC and incidentally the MOSFET which is connected through the Analog Output 0 of the DAC. Outside of this controlling time the DAC will maintain its last state of 0V, meaning the MOSFET and therefore the electrical circuit are open when no measurements are taking place. Simultaneous to the starting of the DAC control cycle the Agilent will start to measure the current that flows through the sensor. In the while loop of the main program a timer is placed with an interval of 30 000 milliseconds. This ensures that there is an interval of 30 seconds between each heating pulse providing ample time for the heater to cool down.

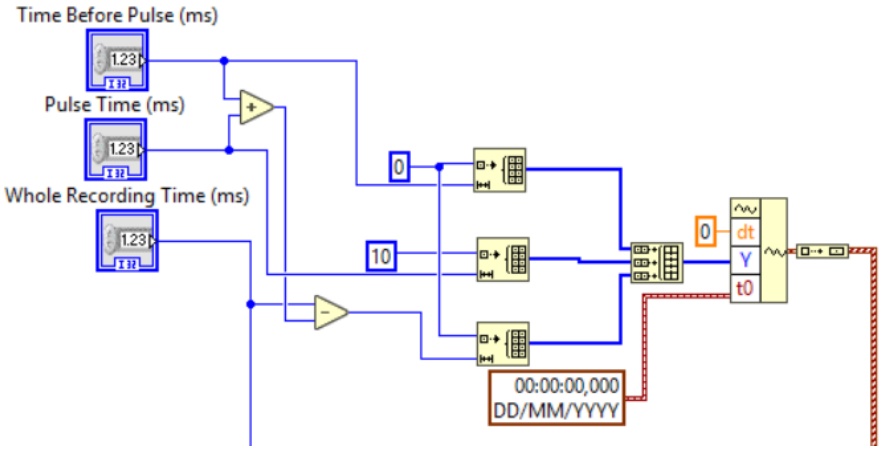

Figure 3-10 Adjustable pulse parameters

Making the measurement file

Existing LabVIEW software for the Agilent 34401A did not support making measurements with intention of saving them to a text file. Therefore extra code was added in order to be able to document all measurements as required. A save path is created after which a new header is made and written to the new text file. In the main program loop the measurement data is added to the text file in combination with the individual time of the measurements. After this process is done the text file is closed. Figure *3-11* shows the program which can be found within the create header Sub Vi while Figure *3-12* shows the code of the program that is required for making the measurement file. Table 3 and Table 4 describe the meaning of the function blocks of Figure *3-11* and Figure *3-12* respectively.

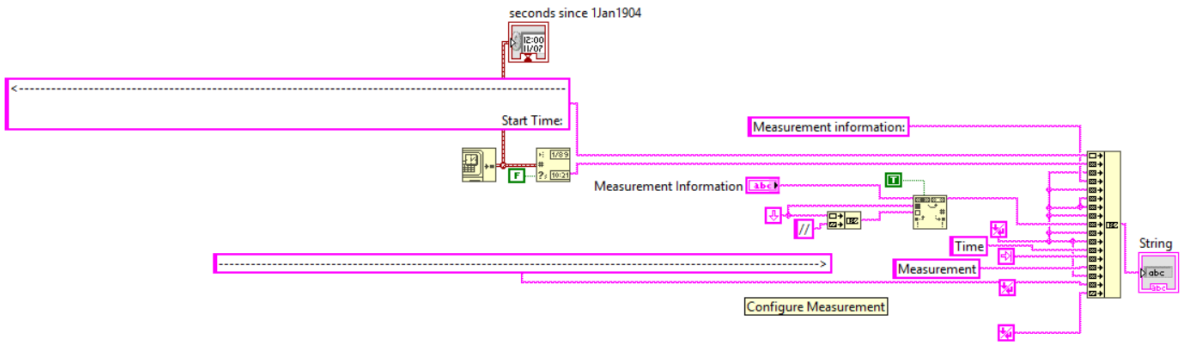

Figure 3-11 Contents of create header Sub VI

Table 3 Overview and function of the program blocks in the Header Sub VI

Function block	Description	Function block	Description
seconds since 1Jan1904	A timestamp function that returns the amount of seconds passed since the 1st of January 1904.	Measurement information:	Data in the format of a string used to form the header.
	Get Date/Time in seconds. Returns a timestamp which is a result of the calculation of seconds since the 1st of January 1904.		Converts a timestamp value or a numeric value to a date and time string.
	Boolean returning true or false value.		Concatenates strings and 1D arrays of strings into a single output string.
	Replaces one or all instances of a substring with another substring.	String	Exports all the output data as data type string.

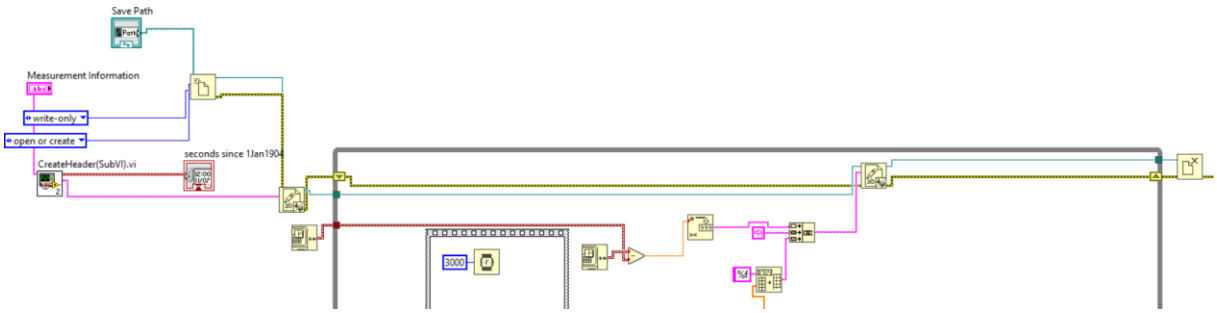

Figure 3-12 Creating and saving text files along with time and measurement data

Table 4 Overview and function of the program blocks of the Agilent program

Function Block	Description	Function Block	Description
	Includes the text from the save path control on the interface as string data type for further use.	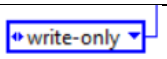	String data with case selection.
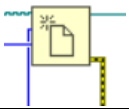	Open, create or replace a file.	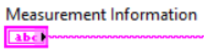	String data as constant.
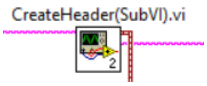	Represents the Create Header Sub Vi.		Writes a string or an array of strings as lines to a file.
	Get Date/Time in seconds. Returns a timestamp which is a result of the calculation of seconds since the 1st of January 1904.		Subtractor, the above incomming value is substracted with the input value below.
	Converts a number to a decimal string of digits.		Converts an array in any dimension to a table string form
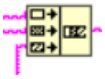	Concatenates strings and 1D arrays of strings into a single output string.		Writes a string or an array of strings as lines to a file.
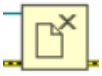	Closes an open file specified by refnum and returns the path to the file associated with the refnum.		Format specifier of the type floating point.
	Wait a specified amount of milliseconds.		

4 Results

4.1 Results capacitive type moisture content sensors

4.1.1 Introduction on characterizations

Al sensors received a base characterization which includes measurements in air & water. Tests that were performed include a double cloth experiment and a ramped relative humidity test. After these tests, other tests took place to determine the susceptibility to ambient conditions.

4.1.2 Double cloth experiment

A test was constructed by soaking a wet textile and then laying it on top of the moisture content sensor. This allows the moisture from the wet cloth to soak into the dry cloth. Since the temperature level is kept constant at 23°C and the relative humidity remained at the standard value of 30% This means not only the soaking in of the fluid but also the evaporation of the fluid from the cloth will be visible in the results from the test. The measurement setup which consists of the LC100-A setup and a scale placed in a climate chamber can be seen in Figure *4-1*.

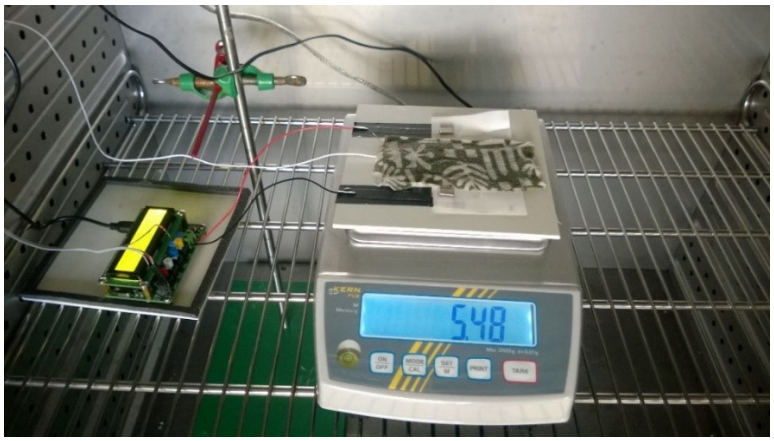

Figure 4-1 Measuring setup; cloth on top of capacitive type moisture content sensor

4.1.3 Susceptibility tests

As mentioned in chapter 2.1.3 the base sensor design contains a part which acts as a relative humidity sensor rather than a moisture content sensor. The base sensor and the altered design which contains an added T_iO_2 layer were compared to see if the added encapsulation layer helped against susceptibility against ambient conditions. As can be seen from a test with the older setup in Figure *4-2*, the range over which could be measured linearly was increased.

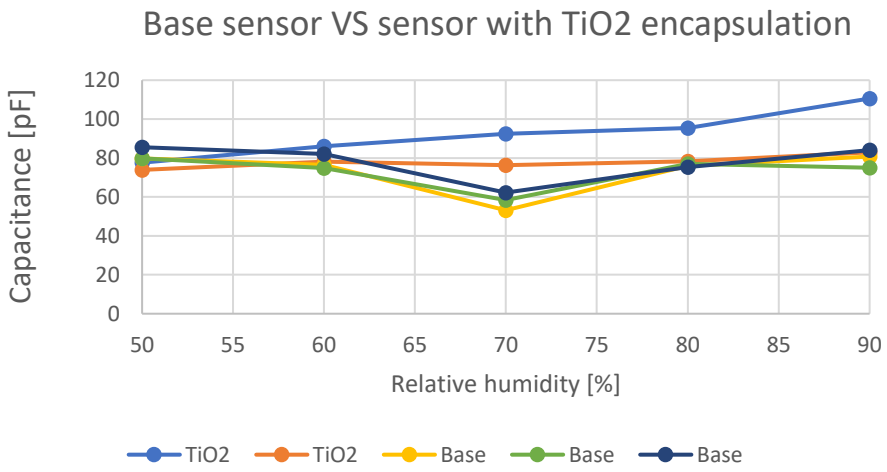

Figure 4-2 Base sensor VS sensor design with encapsulation layer

From the above figure it can be concluded that the added T_iO_2 layer helped against susceptibility towards ambient conditions such as changing RH.

4.1.4 Results of the double cloth experiment

After the textile is placed on top of the sensor the weight drastically increases simply because of the wet cloth being placed on the surface. The capacitance will also increase in accordance to the amount of moisture soaking into the textile of the sensor leading to its moisture content to increase. The temperature remains constant in the climate chamber was programmed to remain 23°C. Due to evaporation the total weight shall decrease over time. This process can be seen in Figure *4-3*.

Figure 4-3 Double cloth measurements

Near the end of the evaporation the weight loss will start to decrease. This is to smaller amounts of moisture remaining to evaporate. At the same time the temperature of the cloth will increase slightly, this is due to the lesser evaporation now needing less heat for the evaporation process. When the evaporation is completely done the weight loss will cease to continue. For the reference measurements below in Figure *4-4*, the sensor used is an Sensirion SHT31 which has an accuracy of 2 %RH and ± 0.2 °C [17].

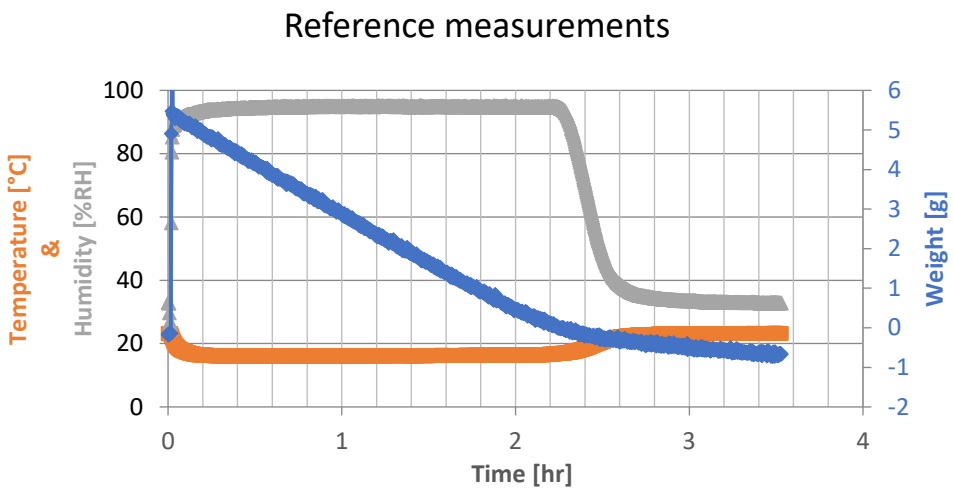

Figure 4-4 Reference measurements for the double cloth measurement

4.1.5 Ramp 40-70% RH

To determine the responsivity of the sensor, a test was performed were steps of 10% RH were performed every ten minutes. It was noted that although the sensor could display the increases and decreases in RH, the capacitance increase between 50-70% RH was notably higher indicating a higher sensitivity in that area. As seen in Figure 4-5 the sensor will gradually increase its value in response to a step of increasing relative humidity. Decreasing steps in relative humidity showed more equally sized steps proving the rate of evaporation is faster than the time it takes for the moisture to be absorbed in the material. This indicates there is a hysteresis that is formed consisting of the time it takes for the moisture to be absorbed and measured and then evaporated again for measuring without being saturated. As seen in Figure *3-4* a fast increase in RH in the form of an immediate step will be displayed as an exponential increase of capacitance. This is due to the fact that there is a physical limit to how fast the textile can absorb the moisture. The relative humidity increase in the climate chamber is faster than the increase of moisture content in the polyester substrate of the sensor.

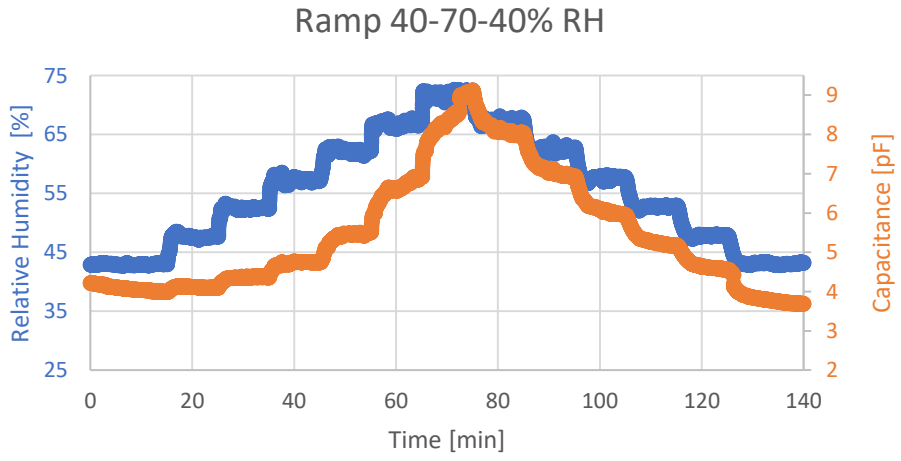

Figure 4-5 Ramp graph

4.2 Results heater type moisture content sensors

4.2.1 Preparation of sensor samples

The micro technical samples needed to be tested in humid environments and even in some cases fully submersed in water. Therefore they needed to be waterproof to a degree were they could be immersed in water.

These heaters are fully encapsulated by polyimide leaving only the connection points of the heater exposed. These are glued to a PCB with conductive glue after which another layer of tape is placed over the front of the connections sealing of the front sides of the heater. The rear has a gap between the heater and the PCB which is glued to prevent water from coming in. The micro technical heaters come in different sizes of surface area which can be seen in Figure *4-6*.

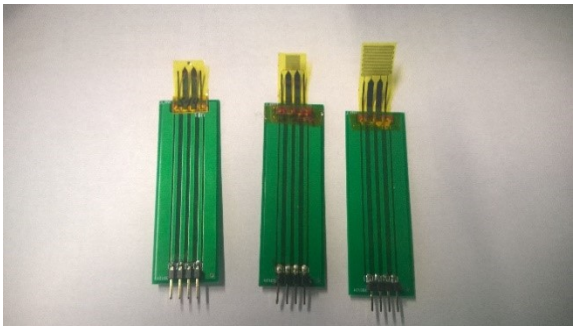

Figure 4-6 Micro technical heaters in 1mm²,25mm² and 100mm² surface area respectively

4.2.2 Preparation printed heaters and self-regulating printed heaters

The printed heaters are printed on polyimide foil with silver ink without any further encapsulation. The encapsulation layer was achieved by applying polyimide tape with a thickness of 50µm over the conductive layer and the connections made with silver glue.

4.2.3 Air-water sensitivity tests and their purpose

As mentioned in chapter 2.2.2 the water content can be estimated by determining the relative resistance change. The relative resistance change correlates to the temperature change as seen in equation 3.2. During this measurement the heaters will be placed in different environments. This will be either in air or fully submersed in water. Both environments vastly differ in conducting heat and heat capacity, leading the heater to heat up differently. By comparing the graphs of the relative resistance changes in both environments a comparison of the measuring range and sensitivity of different sensors can be formed.

4.2.4 Fundamental aspects of the air-water sensitivity test with heaters

During these tests the current is measured and studied. This is similar to previous tests done in the past at Zweibrücken. The resistance can simply be calculated using ohms law displayed in equation 4.1 below.

$$R = \frac{U}{I}\ [\Omega] \tag{4.1}$$

Thermal effusivity takes both heat storing abilities and heat dissipating capabilities such as specific heat capacity and thermal conductivity respectively into consideration. Water is for instance a better heat conductor than air but is also more capable of storing heat leading in it having a higher specific heat capacity [19] [20]. It is for this reason the heater will heat up faster in air. In other words, when a heater is brought into contact with a textile it shall heat up faster when there is less moisture present in the textile.

In Figure *4-7* and Figure *4-8* the full measuring steps in air and water are displayed respectively as datasets. As displayed in Figure *4-7* the current decreases over time in air which means the resistance is increasing. The slope of these decreasing currents is different for both air and water.

This indicates two fundamental aspects in measuring with this type of sensor. First important aspect is based on the principle that when the heater is in contact with a heat conducting material, it will heat up more slowly or its heat might be dissipated entirely. The second aspect is that different materials not only conduct heat differently but also react in various ways to heat. This later aspect includes that for instance water isn't only a better heat conductor then air but heat can also help the water to evaporate because it can detract more heat from the sensor surface as the heater heats up. Models can be formed with proper knowledge of the materials and the heater to determine moisture content in textiles. It should be noted, however, that the very working principle of the sensor aides in evaporating the very moisture it is measuring leading in it altering the exact amount of moisture in the textile.

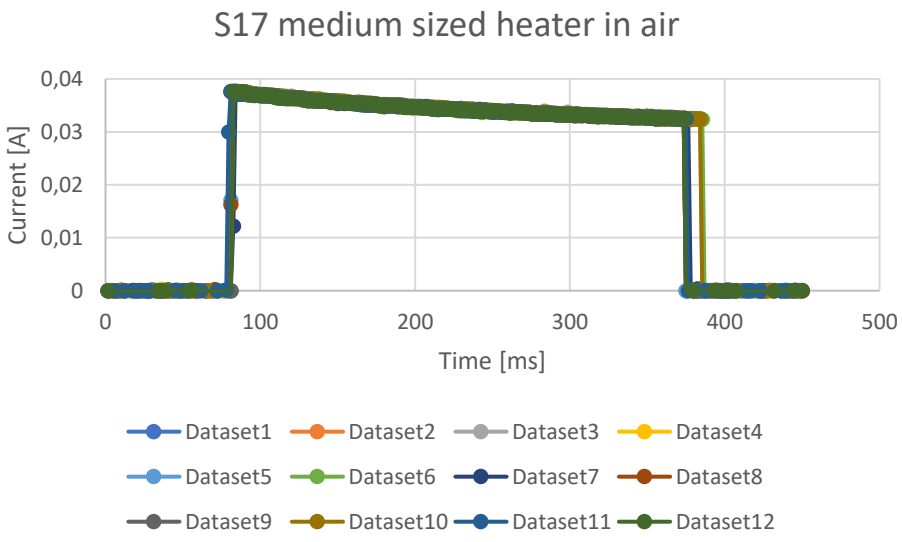

Figure 4-7 Medium sized micro technical heater tested in air

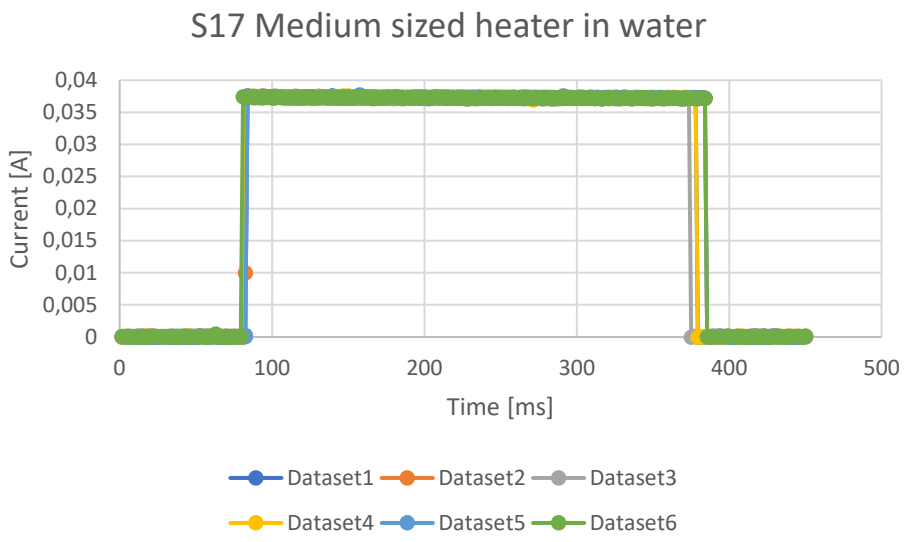

Figure 4-8 Medium sized micro technical heater tested in water

4.2.5 Preparations air-water test

In order to perform this test, the heater must be introduced to a DC voltage step. The step itself is realized by the hardware and LabVIEW program of the heater setup mentioned in chapter 6. To know the amount of samples per second during the measurement and the sample time, the right parameters had to be calculated for the LabVIEW program. A pulse time of 300 milliseconds is set and it is noted that over the entire pulse around 200 samples are collected within the area desired to measure the current change. The amount of samples per second and the sample time can be seen in the calculations below.

Pulse time = 300ms

Collected samples over pulse = 200

Amount of samples per second:

$$\frac{200}{300} = 0{,}66667 \text{ samples/ms}$$

Sample time:

$$\frac{1}{666{,}67\frac{1}{s}} = 0{,}0015s$$

Next the physical parameters of the measurement should be known. Every sensor has a slightly different resistance which means every sensor has to be measured separately by means of 4-wire resistance measurement. To make the test comparable each heater should be introduced to the same amount of power per square millimeter. The chosen amount, as calculated in paragraph 4.2.6, was 25mW/mm². Equation 8.2, which is used to calculate the power over the active surface area ,better known as intensity, can be combined with Ohm's law (equation 8.1) as displayed in equation 8.3.

$$\Upsilon = \frac{U.I}{A} \quad \left[\frac{mW}{mm^2}\right] \tag{4.2}$$

$$\Upsilon = \frac{U^2}{R.A} \quad \left[\frac{mW}{mm^2}\right] \tag{4.3}$$

This leads to the formula to calculate the voltage each individual sensor should receive to have 25mW/mm² power.

$$U = \sqrt{\Upsilon.R.A} \ \ [V] \tag{4.4}$$

4.2.6 Calculating the amount of power for the air-water test

The amount of power per active surface area had to be the same for all sensors in the air-water test in order for the results to be comparable. The temperature increase that would follow from increasing the power is taken into account in the calculations of this paragraph. The information relating to the material properties of the Kapton or used silver ink was found in their respective datasheets [21][22]. These calculations do not take into account any dissipation of heat and are the theoretical maximal temperatures a sensor could reach.

Properties of the used Kapton substrate:

$T_{max} = 400°C \mathrel{\widehat{=}} 673{,}15K$ ρ_{Kapton}= 1,42 g/cm³ $C_{s_{kapton}} = 1{,}09 \ \frac{J}{g.K}$

$T_{start} = 20°C \mathrel{\widehat{=}} 293{,}15K$

Properties known in advance:

$\Upsilon = 25 \frac{mW}{mm^2}$ $t_{Pulse} = 300ms$

$A_{printed\ heater} = 100mm^2$

$A_{mediummicro\ technical\ heater} = 25mm^2$

$A_{large\ micro\ technical\ heater} = 100mm^2$

Calculation of the volumetric heat capacity:

$$c_v = \rho \cdot c_s \left[\frac{J}{K.cm^3}\right] \tag{4.5}$$

$c_v = 1{,}42 \frac{g}{cm^3} \cdot 1{,}09 \frac{J}{g.K}$

$c_v = 1{,}55 \ \frac{J}{K\ .cm^3}$

Calculation of volume of micro technical and printed heater:

$$V = A \cdot s \ [cm^3] \tag{4.6}$$

$V_{medium\ micro\ technical} = 0{,}25cm^2 \cdot 0{,}002cm = 5 \cdot 10^{-4}\ cm^3$

$V_{large\ micro\ technical} = 1cm^2 \cdot 0{,}002cm = 2 \cdot 10^{-3} cm^3$

$V_{printed\ micro\ technical} = 1cm^2 \cdot 0{,}005cm = 5 \cdot 10^{-3} cm^3$

Heat capacity of micro technical and printed heater:

$$C_H = V \cdot c_v \left[\frac{J}{K}\right] \tag{4.7}$$

$$C_{H\ medium\ micro\ technical} = 5.10^{-4} cm^3 \cdot\ 1{,}55 \frac{J}{K.cm^3} = 7{,}75 \cdot 10^{-4} \frac{J}{K}$$

$$C_{H\ large\ micro\ technical} = 0{,}002 cm^3 \cdot\ 1{,}55 \frac{J}{K.cm^3} = 0{,}0031\ \frac{J}{K}$$

$$C_{H\ printed\ heater} = 5.10^{-3} cm^3 \cdot\ 1{,}55 \frac{J}{K.cm^3} = 7{,}75 \cdot 10^{-3} \frac{J}{K}$$

Temperature change per heater:

$$\Delta\vartheta = \frac{1}{C_H} \cdot \int \frac{\Upsilon}{A}\, dt \quad [K] \tag{4.8}$$

$$\Delta\vartheta = \frac{1}{C_H} \cdot \Upsilon \cdot A \cdot\ t\ [K] \tag{4.9}$$

$$\Delta\vartheta_{medium\ micro\ technical} = 0{,}025 \frac{W}{mm^2} \cdot\ 25 mm^2 \cdot 0{,}3 s \cdot \frac{1}{7.75 \cdot 10^{-4}} \frac{K}{J} = 241{,}93\ K$$

$$\Delta\vartheta_{large\ micro\ technical} = 0{,}025 \frac{W}{mm^2} \cdot 100 mm^2 \cdot\ 0{,}3 s\ \cdot \frac{1}{0{,}0031} \frac{K}{J} = 241{,}935 K$$

$$\Delta\vartheta_{printed} = 0{,}025 \frac{W}{mm^2} \cdot\ 100 mm^2 \cdot 0{,}3 s \cdot \frac{1}{7{,}75 \cdot 10^{-3}} \frac{K}{J} = 96{,}77\ K$$

Calculated temperature that each sensor will reach after heating:

$$T = T_{start} + \Delta\vartheta\ \ [K] \tag{4.10}$$

$$T_{medium\ micro\ technical} = 293{,}15K + 241{,}93K = 535{,}08K \mathrel{\widehat{=}} 261{,}93°C$$

$$T_{large\ micro\ technical} = 293{,}15K + 241{,}93K = 535{,}08K \mathrel{\widehat{=}} 261{,}93°C$$

$$T_{printed} = 293{,}15K + 96{,}77K = 389{,}92K \mathrel{\widehat{=}} 116{,}77°C$$

Conclusions:

That calculations show that a larger heater has the same temperature change as its medium sized equivalent. The difference in volume allows the larger heater to tolerate more heat due to having a higher volumetric heat capacity. This makes it more capable in handling a certain amount of power per surface area. Therefore the printed heater was only calculated from its assumed starting size 100mm² as the resulting end temperatures would be the same for all printed heaters introduced to 25mW/mm². It should also be noted that the calculated end temperature does not take into consideration any influences that lead to the dissipation of the heat. This means the temperatures calculated above are the maximum temperatures which the heaters could only theoretically reach under perfect circumstances with no heat dissipation to the ambient surroundings. The Kapton foil can handle temperatures up to 400°C while the silver ink can be cured at temperatures of 130°C without any risk of degrading the ink [21][22]. Further it is known from general knowledge that most silver inks are able to handle temperatures up to 200°C. Seeing as neither of the heaters went over their considered respective maximum temperatures, 25mW/mm² was accepted as the power to be used for the air-water test.

4.2.7 Results from the air-water test

The heaters are now introduced to DC voltage pulses with the specific voltage required per sensor to have a power of 25mW/mm² as explained in paragraph 4.2.5. During the test the measured current will change leading to the calculated resistance from each measurement sample to be different. By comparing it to the original resistance value measured by 4-wire measurement the relative resistance change can be calculated as seen in equation 4.11.

$$\frac{\Delta R}{R} = \left(\frac{R_{actual} - R_{original}}{R_{original}}\right) \cdot 100\ [\%] \tag{4.11}$$

This relative resistance change can be used to determine the temperature change. According to formulae 2.4 temperature change is in function of the water content in the textile.

When the results for the relative resistance changes in air and water are subtracted from each other, the resulting graph will be an indicator for the sensitivity of each individual sensor. The previous graphs for medium sensor S17 are shown in Figure *4-9*. The bigger the surface area between the lines of relative resistance change in air and water, the greater the measuring range. The subtraction of air and water measurements can be seen in Figure *4-10* which is used for comparing its sensitivity to that of other heaters.

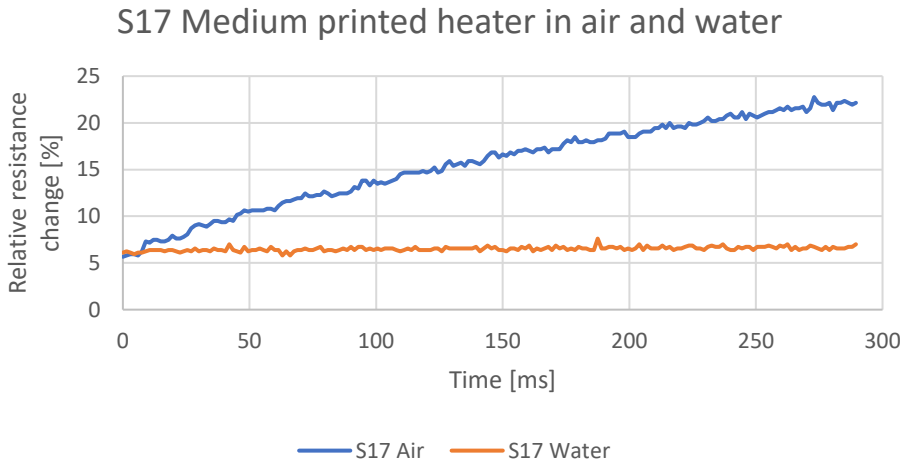

Figure 4-9 Relative resistance changes in air and water

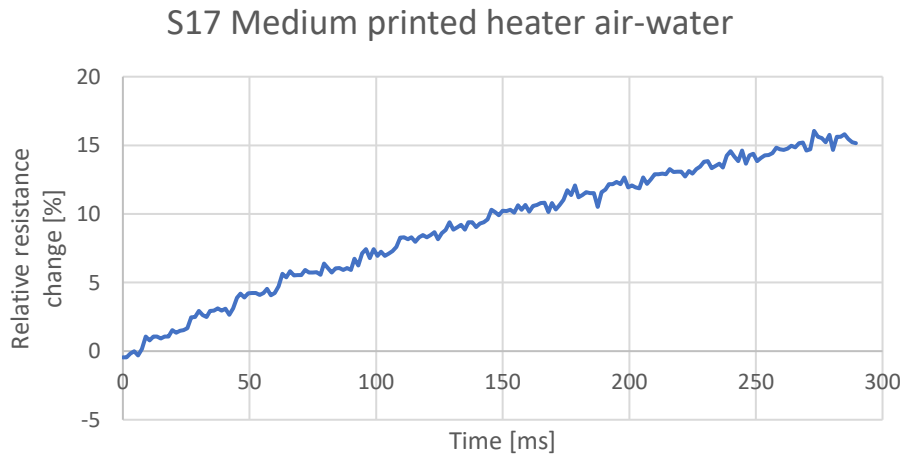

Figure 4-10 Sensitivity of a medium sensor determined from the air-water test

The more fluent the line, the less noise a sensor has during its measurements and the more sensitive the sensor. This was tested for small micro technical heaters on thin and thicker polyimide foil with total thicknesses of 20µm and 127µm respectively. As can be seen in Figure *4-11*, the thinnest sensor is more sensitive and shows increased measuring range compared to the heater with on the thicker foil. It may however, be more susceptible to noise.

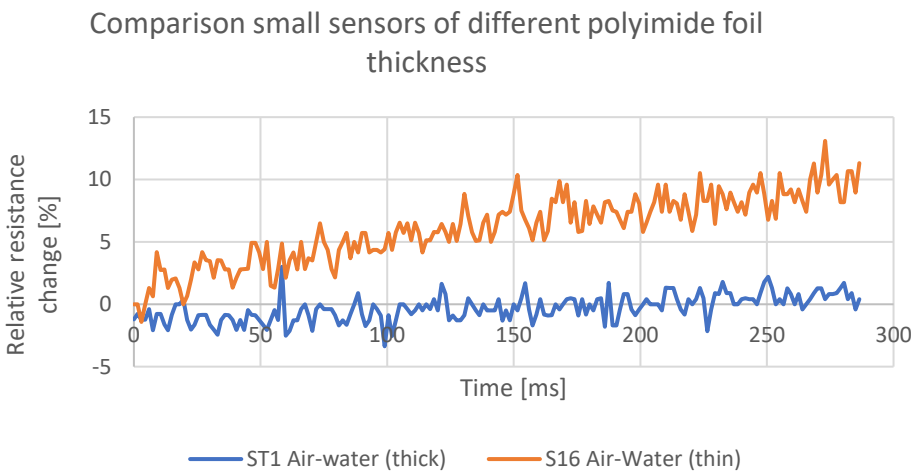

Figure 4-11 Air-water test for thick and thin small sensors

Note that this is only comparable between sensors of the same surface area. Sensors with bigger surface areas need more current and voltage per square millimeter in order to achieve the desired power per square millimeter. The bigger the size of the sensor, the more sensitive it shall be as seen in Figure *4-12*.

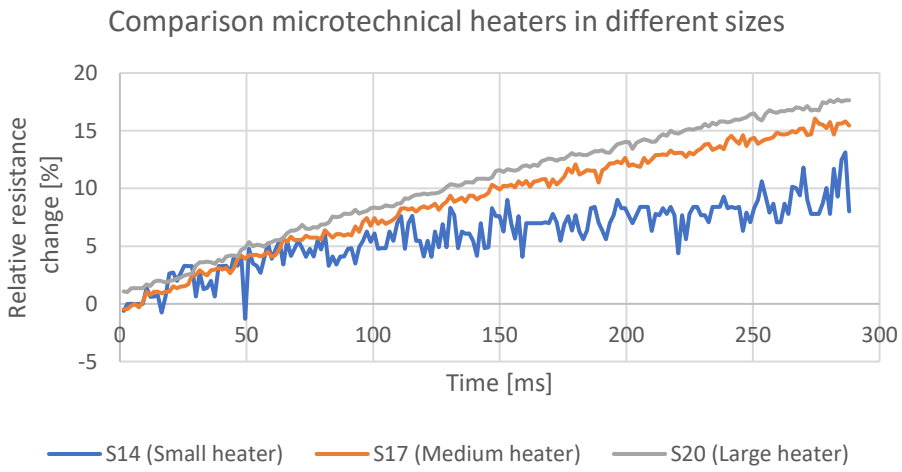

Figure 4-12 Sensitivity of microtechnical heaters in different sizes according to the air-water test

In the fore mentioned figure, the smaller sensor shows more noise than the other sizes. However just increasing the power will not help in the case of a sensor which surface area is 25 times smaller the second smallest size and even 100 times smaller than the largest sensor. The sensor is limited to how much power it can receive because of the amount of heat it must be able to tolerate without reaching temperatures which will damage the heater. Experimenting with the smaller heater shows that doubling its power has nearly no effect on the amount of noise present or increase in sensitivity in the output signal, as can be seen in Figure 4-13. The higher amount of power introduced to the sensor leads to the measurement line starting from 18% instead of 0% relative resistance change in the aforementioned figure. The earlier conclusions indicate that in order to achieve the desired accuracy the choice of the sensor size is of great importance and has to a certain degree higher influence than simply altering the power of the heater.

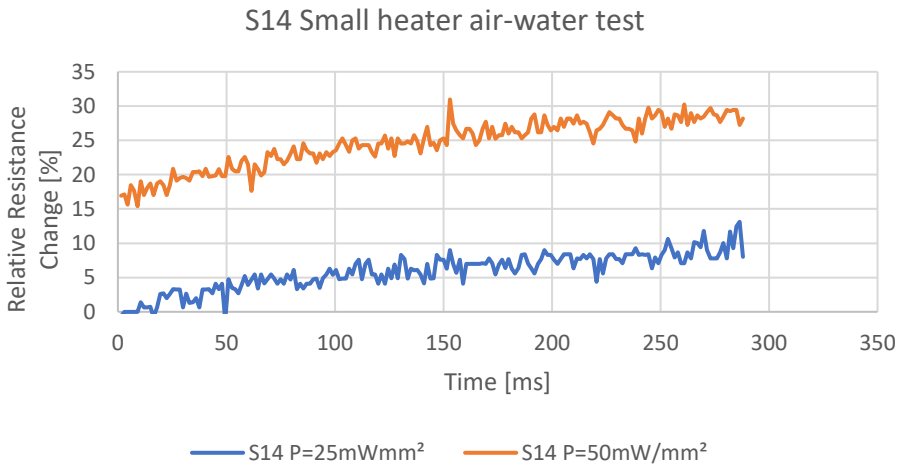

Figure 4-13 Sensitivity of a small sensor at different power levels

The printed heaters shown in Figure 4-14 achieve a sensitivity about half of the microtechnical heaters seen in Figure 4-12. The origin of this can be found in the differences in their design including a difference in thickness. As established by the test seen in Figure 4-11 performed on small microtechnical sensors with different thicknesses in Polyimide foil, the thinner the foil, the better the sensitivity.

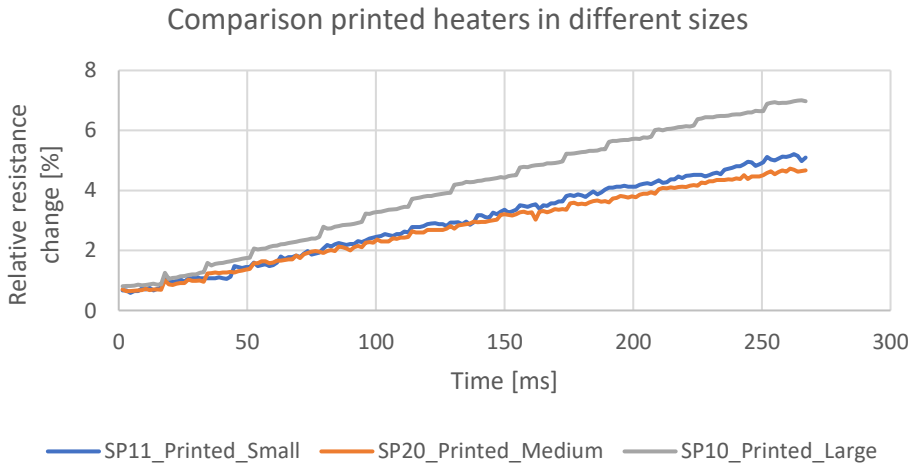

Figure 4-14 Sensitivity of printed heaters of different sizes according to the air-water test

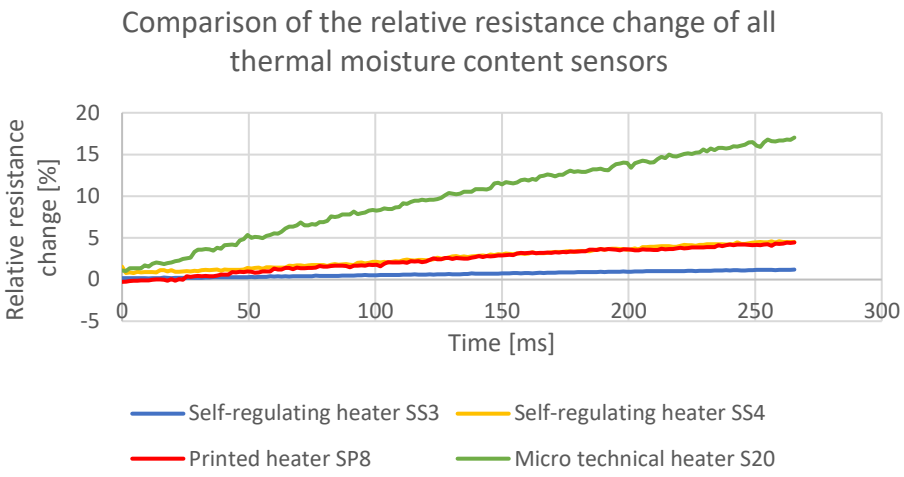

Figure 4-15 Air-water test on all heaters

Figure 4-15 displays all the different heaters with a surface area around 100mm². It becomes apparent that the microtechnical heaters have the best sensitivity. The main advantage they have is that they are a lot thinner than the other variants, as was discussed earlier in the case of Figure *4-11*. The regular printed heaters were printed on a foil of 75µm thick while the self-regulating heater SS3 is 125µm thick with an added polyimide tape encapsulation of 50µm thickness. The microtechnical heaters on the other hand manage to achieve a total thickness just over 20µm. This correlates with what Figure *4-11* proved regarding thinner sensors having better sensitivity. It should however be noted that self-regulating heater SS4, which had a thickness of 140µm, managed to perform as well as heater SP8. Further testing should be performed in the future to know for sure as to why this heater performed better during the test.

4.2.8 Results from susceptibility tests

Similar to how the capacitive type moisture sensors were tested to influences from relative humidity, the heater type moisture sensors were tested for their susceptibility to changes in temperature. This was done by performing an air-water test on a regular printed heater and microtechnical heater. The size of these heaters was 153,94mm² and 100mm²for both fore mentioned heaters respectively. The air-water test was performed in a climate chamber for the measurement in air and in a heated beaker of water for the testing while submersed in water. The used temperatures started at 25°C and went to 40°C in steps of 5°C.

It was noted that for all the tested heaters the values of the measurement sets increased by increasing temperature in both water and air as seen in Figure *4-16* and Figure *4-17*. In separate measurements in air and water at varying temperatures the relative resistance increase was still highest in air due to water being the better water heat conductor. When looking at these individual measurements which can be seen in Figure *4-18*, Figure *4-19*, Figure *4-20* and Figure *4-21*, the influence of the temperature increases can be seen as the curves of the individual start to move upwards due to the nature of the positive temperature coefficient material.

These measurements and calculations were made keeping in mind the principle described in paragraph 2.2.2. The reference resistance used was the resistance measured at 20°C with a 4 wire measurement. This allows the increase of the sensors temperature due to the influence of external temperature changes to be noticeable.

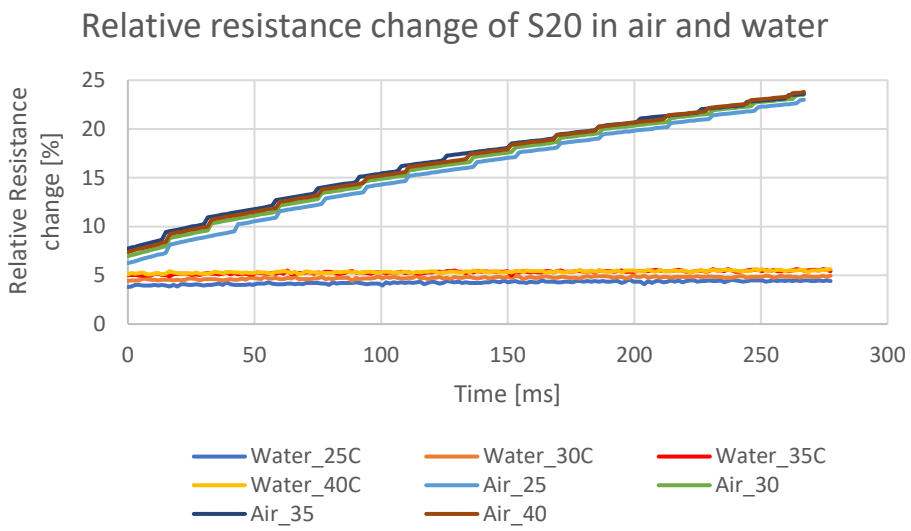

Figure 4-16 Susceptibility test of microtechnical heater S20 in air and water

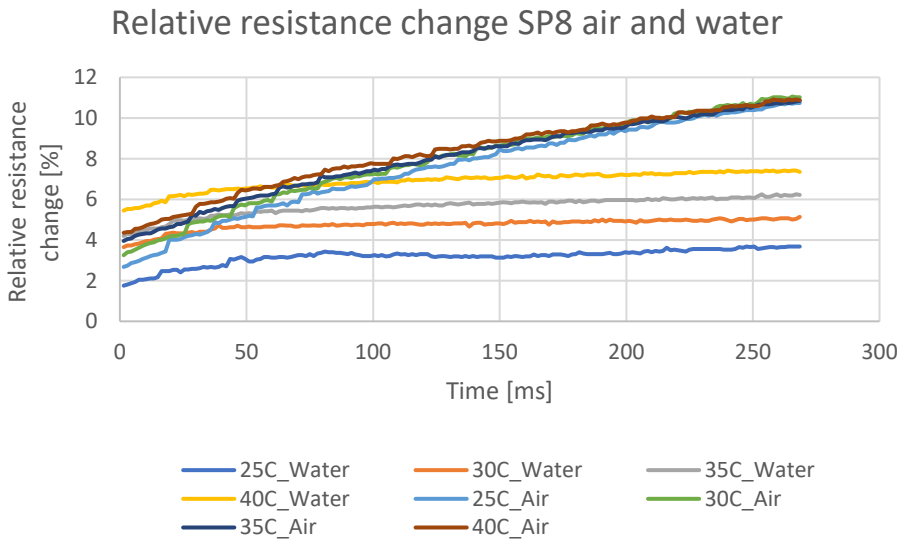

Figure 4-17 Susceptibility test of printed heater SP8 in air and water

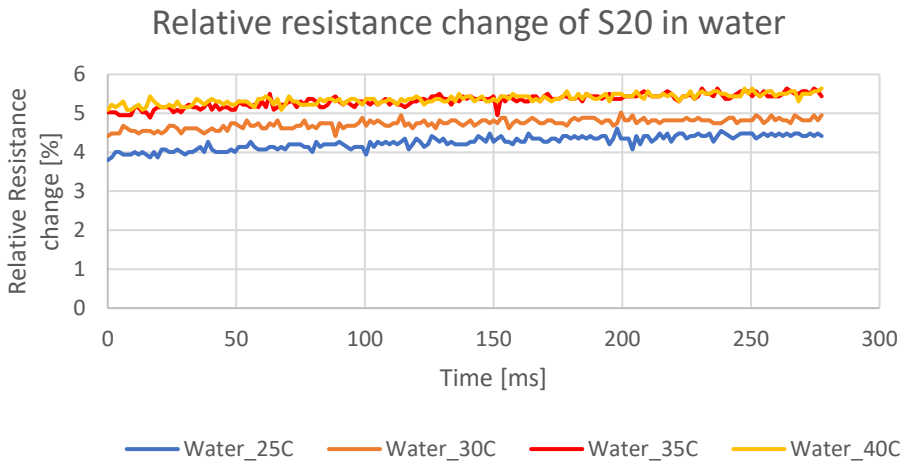

Figure 4-18 Susceptibility test of microtechnical heater S20 in water

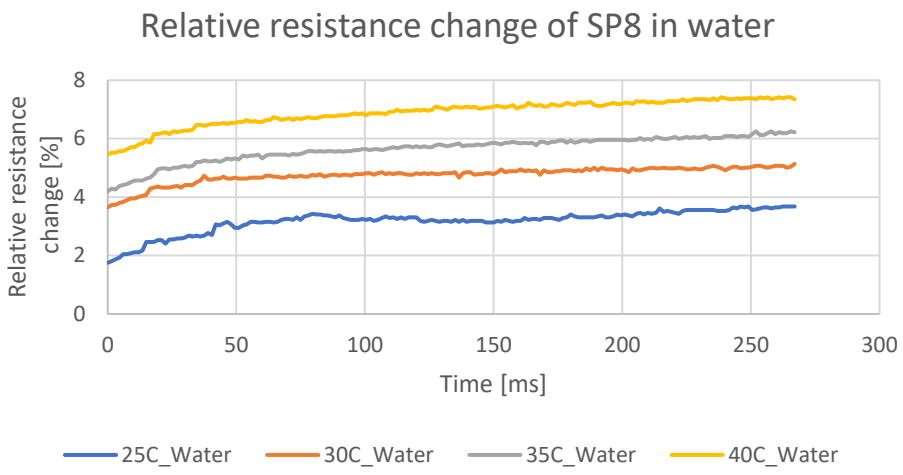

Figure 4-19 Susceptibility test of printed heater SP8 in water

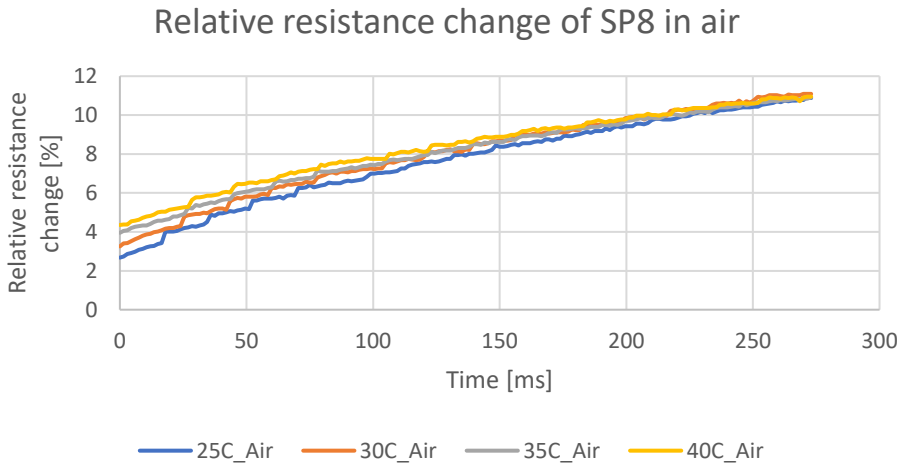

Figure 4-20 Susceptibility test of printed heater SP8 in air

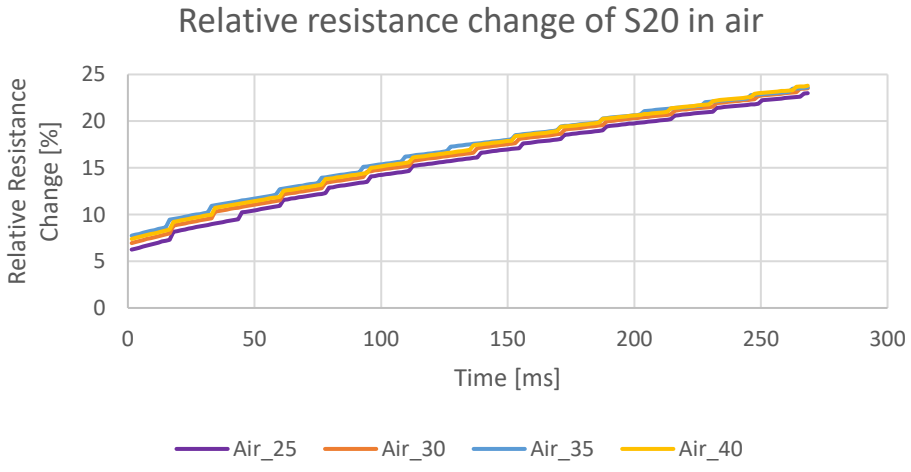

Figure 4-21 Susceptibility test of microtechnical heater S20 in air

4.2.9 Results from cloth test

Similar to the cloth test performed on the capacitive type moisture content sensor, a cloth test was performed on both the microtechnical and the regular printed heater. Once again, a wet cloth would be placed on the sensor and evaporate in the controlled environment of the climate chamber with a relative humidity level of 50% at 23°C. This had as goal to monitor how well the sensors would monitor the changing of the amount of moisture in the cloth it evaporated.

Figure *4-22* and Figure *4-23* display the results of a cloth test of both a printed heater and microtechnical heater in sizes of 153.94mm² and 100mm² respectively. The used cloth had a surface area of 10cm². Similar to the cloth test of the capacitive sensor, the weight continued to decrease until there was no moisture left to evaporate in the cloth. During the evaporation more moisture was replaced with air, which is a better thermal insulator which lead to an increase in resistance of the positive thermal coefficient material of the heaters. This means that the relative resistance shall increase over the period of time during which the amount of moisture in the cloth lowers. The greater the relative resistance change, the more sensitive the sensor. This does exclude certain high peaks or valleys as these tend to be measurement errors. Seeing as these errors are present with both sensors, it can be assumed that the origin of these errors might be because of a temporary disfunction in the measurement setup or one of its components.

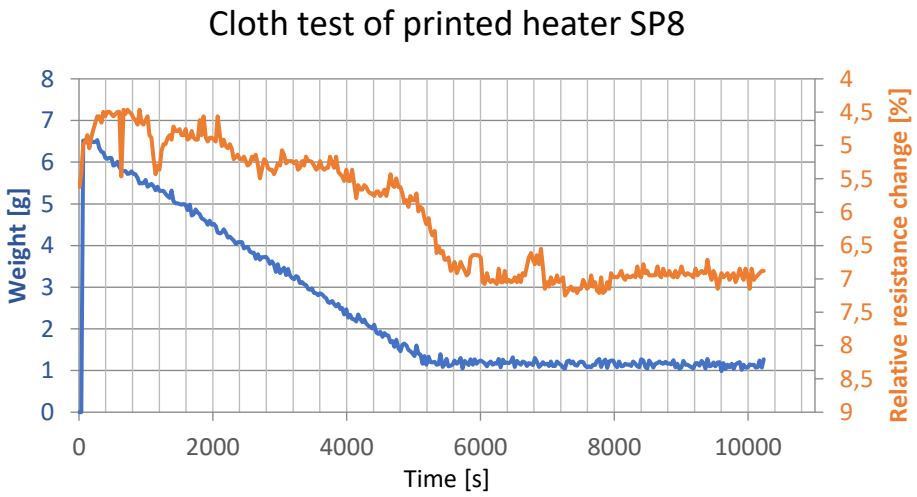

Figure 4-22 Cloth test of printed heater SP8

It is noticeable that towards the end of evaporation both heaters display a sharp increase of relative resistance change. At the moment there is not enough data to form a solid conclusion as to the origin of this phenomenon and it should be further researched. What can be said for sure is that the interval between heat pulses was set to 30 seconds which means the heaters would not heat up continuously because of a lack of cool down time.

The total change in relative resistance is higher in the microtechnical heater which measures from 5,2% to 17,2% versus the change of the printed heater which presents a change from 4,5% to 7,2%. This leads to a total relative resistance variation of 12% and 2,7% respectively. This difference in sensitivity goes hand in hand with what was discussed in chapter 4.2.7 and what was displayed in Figure 4-15, were results also showed the microtechnical heater to be three times more accurate.

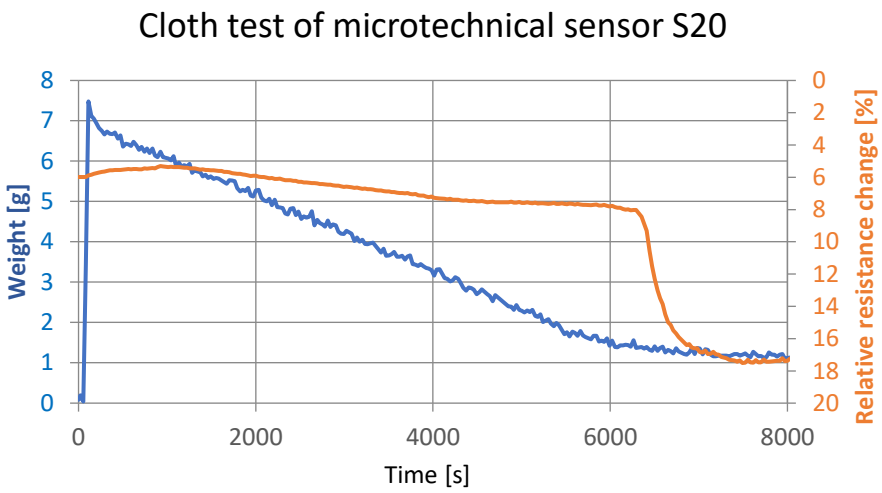

Figure 4-23 Cloth test of microtechnical heater S20

4.2.10 Results from thermal images

Al micro technical and printed heaters were compared under the thermal camera to study the heat up pattern and homogeneity of the heat dissipation over the heater structure. The comparison of micro technical and printed heaters can be seen on the next page in Table 5. In this table heaters of various sizes are compared. The datasheet of the used thermal camera can be found in the appendices.

As seen in Figure 4-27 micro technical heaters produced in a square meander shape show to have more heat in the middle than at their corners. This leads to the amount of heat being higher at the center of the heater. The printed heaters, which have a round shape, do not have this problem. However, the printed heaters have a different issue due to the nature of the production method. Screen printed conductive lines are not as homogeneous and perfectly shaped as the micro technical conductive lines. This leads to small areas in the conductive tracks were the temperature is lower. These ‘cold spots’ can be seen in particular in SP17 which is a medium sized printed heater. The reason of these imperfections is because of imperfections in the screen printing. When the distance from the screen and the pressure are not constant for the whole surface area the ink will have different heights along the print this was proven by Dektak measurements in paragraph 4.2.11.

Table 5 Overview of different heaters in varying sizes

Temperature scale	Micro technical heater	Regular printed heater
Hot Cold Figure 4-24 Temperature scale	**Small** (Sensor number: S16) 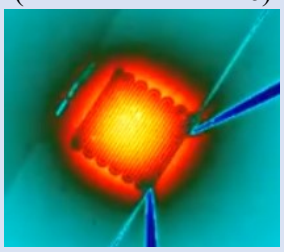 Figure 4-25 Thermal image small sized micro technical heater Hottest temperature: 40.5°C Coldest temperature: 19.9°C	**Small** (Sensor number: SP11) 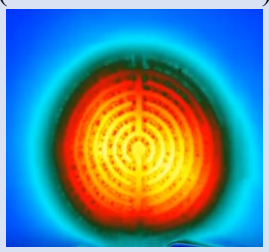 Figure 4-26 Thermal image small sized printed heater Hottest temperature: 39.5°C Coldest temperature: 20.7°C
	Medium (Sensor number S21) 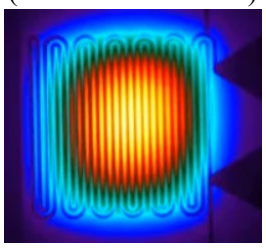 Figure 4-27 Thermal image medium sized micro technical heater Hottest temperature: 135.3°C Coldest temperature: 43.3°C	**Medium** (Sensor number SP17) 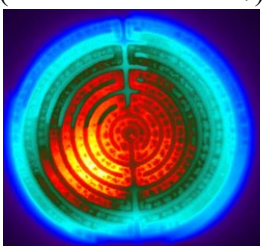 Figure 4-28 Thermal image medium sized printed heater Hottest temperature: 78.0°C Coldest temperature: 23.7°C
	Large (Sensor number S19) 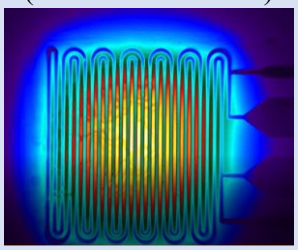 Figure 4-29 Thermal image large sized micro technical heater Hottest temperature: 76.2°C Coldest temperature: 24.3°C	**Large** (Sensor number SP10) 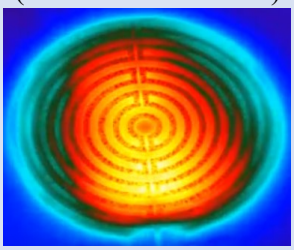 Figure 4-30 Thermal image large sized printed heater Hottest temperature: 44.8°C Coldest temperature: 21.4°C

4.2.11 Heater build and performance evaluation

Oven test

Both printed and microtechnical heaters were tested in an oven that was heated until 100°C. During the course of the test the resistance was measured by means of an Agilent 34401A multimeter. In Figure *4-31* and Figure *4-32* this resistance measurement takes place while a PT100 temperature reference sensor was used to log the temperature. The temperature coefficient α determines the relative resistance increase of the material. The relative resistance increase per temperature change that are used to calculate the temperature coefficient can be seen in equation 4.12 [10].The functions of the trendlines of the respective graphs was set out and they showed that the microtechnical heaters had a slightly higher temperature coefficient of 0,0016 K^{-1}compared to the 0,0014 K^{-1} of the printed ones. The temperature coefficient of silver is slightly higher than that of gold 0,003819 K^{-1} versus 0,003715 K^{-1} [23].

$$\alpha_0 = \frac{\Delta R/R_0}{\Delta \vartheta} \tag{4.12}$$

The measured values are lower than the reference values for the pure materials which means that the temperature coefficient of the material was lowered. In the case of the printed heater, the oven test was performed until 130°C. This was done to make sure there were no bonding materials left in the case of improper curing as the presence of bonding materials might influence the thermal coefficient. A reason as to why the thermal coefficient was lowered for both sensors was found in an article by F.Warkusz [24]. In this article it was concluded that for firmly attached films with a different thermal expansion coefficient between the film in question and the substrate, the thermal coefficient of resistance is influenced by thermal strain. With increasing film thickness and grain diameter the strain coefficients of the film tend to strain the coefficients of resistivity for the bulk of the material.

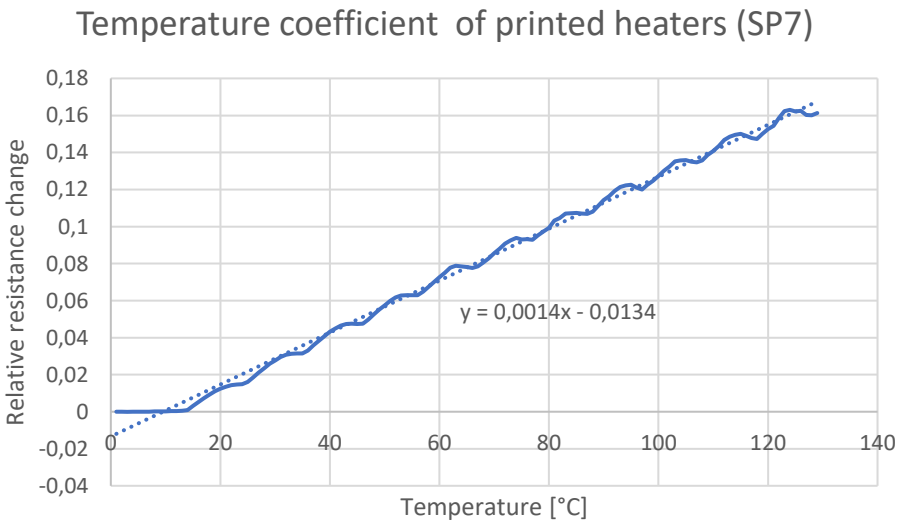

Figure 4-31 Temperature coefficient SP7

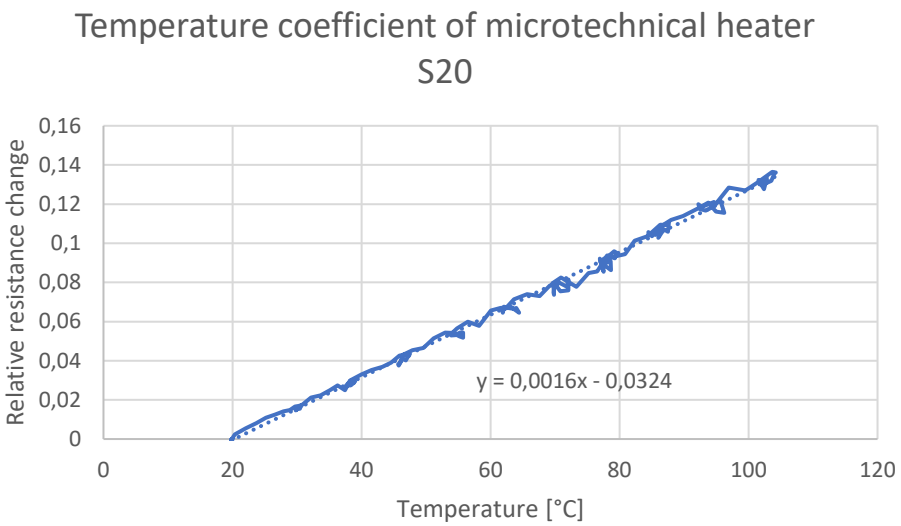

Figure 4-32 Temperature coefficient S20

Dektak surface measurements

The conductive tracks of the screen printed heaters showed inconsistency in their shape and height under the microscope. An inconsistency in the conductive lines can be seen on Figure *4-34* and Figure *4-35* displays an ink insufficiency in a printed heater, potentially due to not enough ink remaining on the screen of the screen printer or corona treatment that was performed in order to increase surface energy. In order to measure the roughness of the ink of the conductive tracks, Dektak measurements were performed on the heaters.

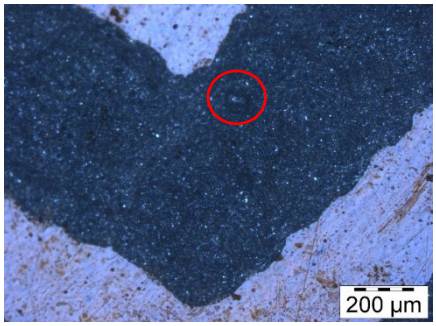

Figure 4-33 Microscope image of printed heater SP12

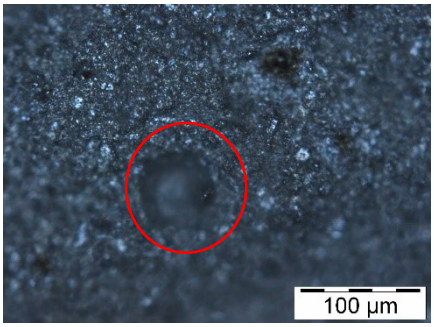

Figure 4-34 Inconsistency in thickness

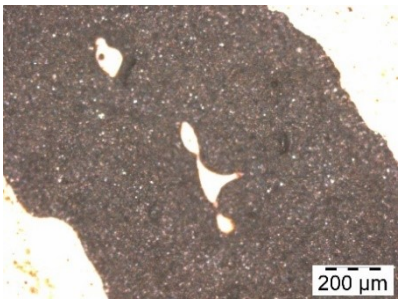

Figure 4-35 Ink insufficiency in printed heater SP7

Comparison of single conductive lines

The conductive tracks of the printed heaters were measured both in horizontal and vertical direction. Two of the vertical lines will be discussed. In Figure *4-36* and Figure *4-37*, the third and fifth conductive lines can be seen. The conductive lines showed multiple spikes. The most extreme case showed a 15µm difference between the lowest and highest point while the smallest peak showed a difference of 7µm.

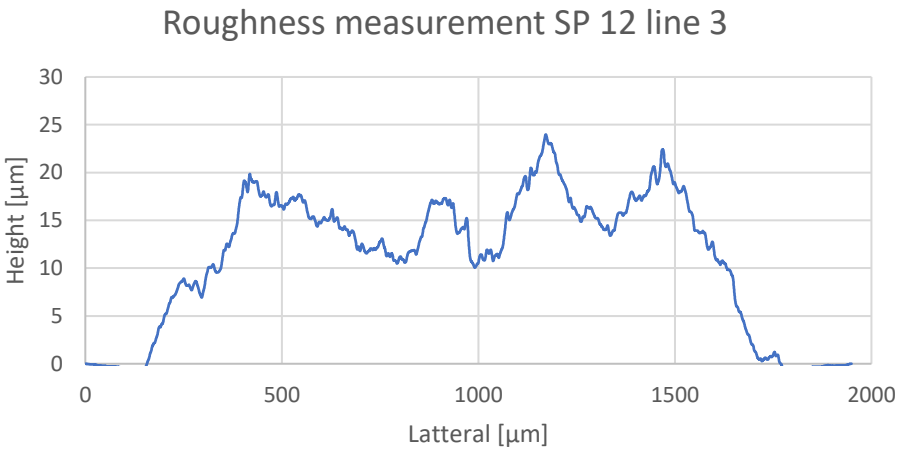

Figure 4-36 Roughness measurement printed heater SP12 line 3

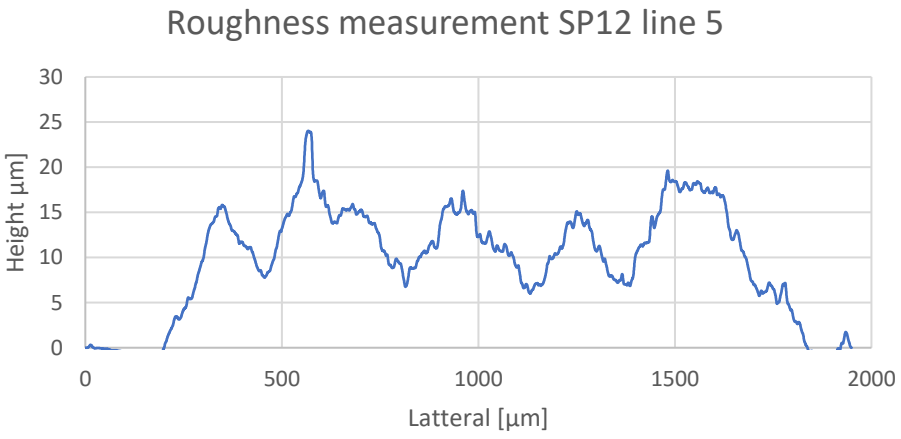

Figure 4-37 Roughness measurement printed heater SP12 line 5

Measurement over multiple conductive lines

A measurement over several conductive lines and the Polyimide foil between these lines was performed. It should be noted that the sample could only be taped from the sides in order to flatten its surface for the measurements. This was due to avoid damaging the ink or hindering the measuring stylus' movement. What becomes apparent from these measurements is that the foil surface is a lot smoother than the ink's surface. This leads to the conclusion that the foils' roughness is not the reason of the differences in roughness found in the conductive lines. Instead the origin of the problem can be found in the ink having different roughness's.

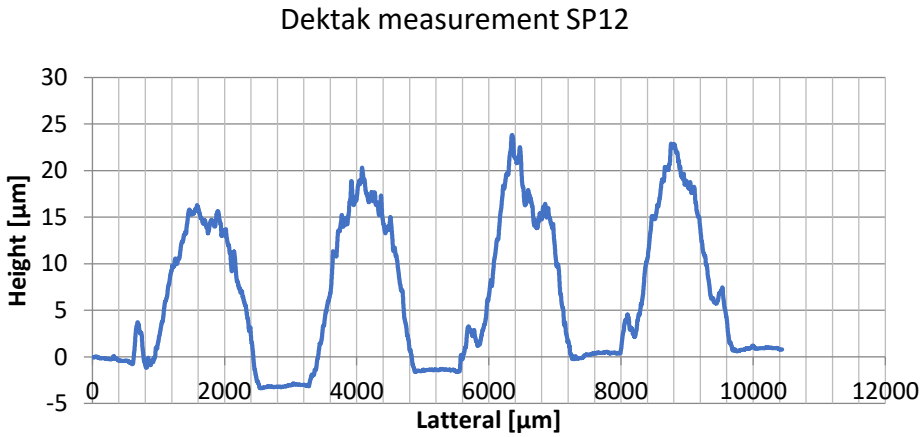

Figure 4-38 Printed heater SP12 vertical Dektak measurement

Overview of Dektak measurement values SP12

A general overview from the Dektak measurements can be found bellow in Table 6. It must be noted that individual vertical lines have similar properties. However, by performing a total surface measurement in horizontal direction it becomes apparent that the ink is not consistent in surface roughness over the entire surface. This is supportive to the theory that the distance from the screen and pressure when not constant over the whole surface while screen printing can lead to different heights in the printed conductive lines as mentioned earlier in paragraph 4.2.10.

Table 6 Overview of results from surface measurements

Measurement	Vertical line 3	Vertical line 5	Horizontal total
p_a (Roughness average) [µm]	5,34	4,33	10,02
p_v (Maximum Valley Depth) [µm]	12,59	12,68	17,29
p_t (Maximum height) [µm]	24,74	26,05	52,74

5 Conclusion and discussion

5.1 Measuring setups, the importance of continuous improvement

5.1.1 LC-100A capacitance measuring setup

As mentioned in chapter 3.1 the LC-100A is a device that measures capacitance. It was required for the device to measure in the picofarad range which requires high accuracy. Therefore great effort went into making the setup as reliable and accurate as possible. This was obtained in two ways, the realization of continuous measurements over longer periods of time and the improvement of the setup in general.

Firstly, by being able to connect the LC-100A to a computer and using a LabVIEW program, continuous measurements could be achieved. This led to a greater amount of data for evaluation of sensor performance which could be compared in order to achieve greater overall reliability in the measuring method.

Secondly, the overall construction of the setup was altered in a way that required shorter cables and connected the sensor directly to two copper attachments. This gave way to more accurate results of sensor performance as explained in chapter 3.1.4.

5.1.2 Measuring setup for heater type moisture content sensors

The measuring setup for heater type moisture content sensors utilizes an Agilent 34401A multimeter to measure the current during the heat up of a sensor as explained in chapter 3.2. This is an improved version of the former measuring setup meant for measuring microtechnical sensors. In this original setup a quarter Wheatstone bridge was used leading to a limitation in measuring sensors with resistances of different magnitudes. In order to make the setup more useable it had to be able to measure sensors of various resistances. To achieve this, the setup was changed to work without the quarter bridge and directly implement the Agilent 34401A as seen in Figure *3-7*.

The direct adaptation of the Agilent multimeter in the measurement setup led to more flexibility but in order to make proper use of the multimeter and the setup, a LabVIEW program had to be made. The used program consists of already existing Sub-VI's which were made specifically for the multimeter and added code. This added code was needed to control the time during which the MOSFET was closed, introducing the sensor to a current for the heating cycle. Simultaneously with the closing of the electrical circuit via MOSFET, the added code started current measurement with the Agilent which could be adjusted in measuring range such as Amps or milli amps. The total improvements lead to the flexibility needed to be able to measure sensors with different resistances such as the regular printed heaters in various sizes and self-regulating printed heaters.

5.2 Constructive improvements and alterations to the sensors

5.2.1 Improvements on the design of the capacitive type moisture sensors

As mentioned in paragraph 2.1.3 alterations were made in the form of an added TiO_2 layer. This was done to make the capacitive sensor less susceptible to ambient changes by encapsulating it from the ambient. It was proven that this alteration increased linearity over longer ranges while lowering ambient influence of relative humidity as discussed in paragraph 4.1.3 and shown in Figure *4-2*. This made the sensor more usable for a variety of conditions and applications due to increased measuring performance.

5.2.2 Constructive alterations for testing with heater type moisture sensors

The heater type moisture sensors were altered for increasing testability. For instance the microtechnical heater was glued with conductive ink on a PCB and was made waterproof by means of Polyimide tape and electrically conductive glue. This resulted in a sensor application perfect for immersing applications where the sensor had to be fully immersed in water.

The printed heaters received similar treatment by gluing on connection wires and taping polyimide tape over their conductive lines to prevent water from entering and shortcutting the sensor. These similar protective measures on the sensors formed an ideal base for usage in air-water tests.

5.2.3 Conclusions of measurements

Air-water test

The air-water tests proved to be a great method to compare and evaluate various heater type moisture content sensors. Whilst this paragraph servers to discuss the results of the air-water test as a whole, the individual discussions of the results can be found in paragraph 4.2.7. An overview of the graphs correlating to the upcoming conclusions can be found below in Figure *5-1*.

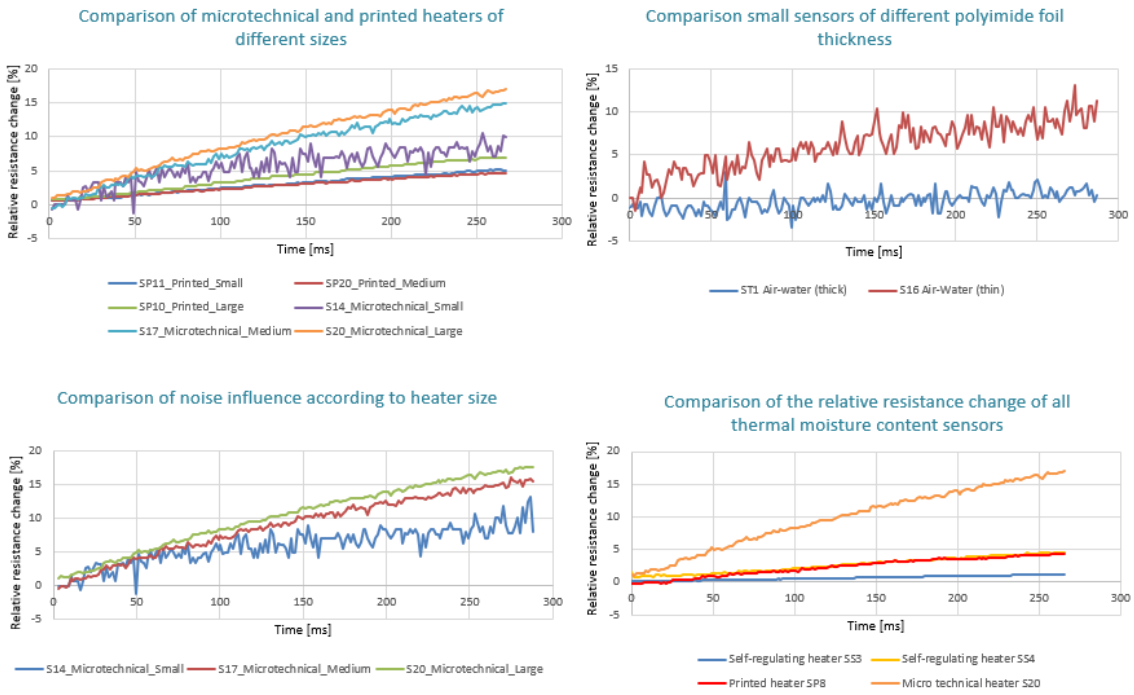

Figure 5-1 Overview of graphical results of the air-water test

Influence of thickness

When microtechnical heaters of different thicknesses were compared, the thinnest version showed to be more accurate. This result was again proven in a similar comparison between different types of heaters which all had an active surface area around 100mm². In all cases excluding one the thinner heaters performed better than their thicker counter parts. This result found in the graph "Comparison of the relative resistance change of all thermal moisture content sensors" of Figure *5-1* correlated to what Figure *4-11* displayed, supporting the theory that thinner sensors are more sensitive.

Influence of size

An air-water test was performed on printed and microtechnical heaters in sizes ranging from small to large. This can be seen in the graph "Comparison of microtechnical and printed heaters of different sizes" of Figure *5-1*. Once again the thinner sensors performed better but what was noticeable, was that the larger sizes generally performed better than the smaller sizes. This was most noticeable with the microtechnical heaters where the smallest heater was 25 times smaller than a medium heater and a 100 times smaller than its large equivalent. In the case of the printed heaters the medium heater is only 62,63% bigger than its small equivalent while the large heater is 10,8 times bigger. This leads to the difference in measurement values being more decisive in the case of the large heater.

Noise

The smallest heater that was tested, was a 1mm² microtechnical heater. In all graphs were small sized microtechnical heaters were used in Figure *5-1* an amount of noise can be noticed. Due to their smaller size the sensors cannot be introduced to a high current because they are limited in the amount of power they can dissipate. The calculations that were used to empower the sensors with 25 milli Watts per square millimeter can be found in paragraph 4.2.6. Increase of size ,then, can lead to more sensitivity while a decrease in size can lead to noise. Size is thus an important parameter to keep in mind when designing and building a thermal type moisture content sensor.

Cloth and double cloth test

The double cloth test is explained in paragraph 4.1.2. During this test, the results, which can be found in paragraph 4.1.4, displayed how the capacitive sensor was able to measure the change in moisture content. It measured continuous lines of the process that displayed how the capacitance increased when moisture entered the cloth and decreased by evaporation.

The cloth test with thermal moisture content had the benefit that it didn't require the water to be adsorbed in the textile upon which the sensor was printed. The fact that this sensor is a standalone unit that can be brought into contact with the textile and measure real time is a considerable benefit. The printed capacitive sensor can only make up for this in the case it is printed directly on the textile which is desired to be measured.

Further as mentioned in paragraph 4.2.9, the heaters were able to display a changing relative resistance in accordance with the changing moisture content levels. The sensitivity of the types of heaters, however, varied greatly. Similar to what was found and concluded in paragraph 4.2.7 in accordance with the results of the air-water test, the thinner microtechnical sensors showed greater sensitivity.

Susceptibility tests

Susceptibility tests were performed on both the capacitive- and thermal type moisture content sensors to research the influence of ambient conditions. For the capacitive type sensors this meant introducing them to changes in relative humidity while the heaters were introduced to environments of varying temperatures.

In paragraph 4.1.3 the base design of the capacitive sensors was found to be influenced by relative humidity. Under normal circumstances, the measurements of the sensor should have displayed a linear increase in capacitance as the moisture is adsorbed in the material. However, this was not entirely the case which entailed a need for a solution which safeguarded the capacitive working between the conductive layers. A solution was found in an encapsulating T_iO_2 layer which did not disturb the capacitive workings of the sensor as discussed in paragraph 2.1.3. Measurements proved to be more linear and the linear measuring range was improved from 70-90% to 50-90% as shown in Figure *4-2*. It should be noted that these measurements were taken only with the old measuring setup which is not as accurate as the one made later on discussed in paragraph 3.1.4. However these results were found to be true for multiple sensors within the same test.

The possible susceptibility of the thermal moisture content sensors was tested by performing an air-water test in environments of changing temperature. The air test was performed in a climate chamber with 50% relative humidity and the temperature was altered from 25°C to 40°C in steps of 5°C. Similarly the part of the test performed immersed in water was performed under temperatures ranging from 25°C to 40°C with steps of 5°C. An overview of these measurements can be found in Figure *5-2*.

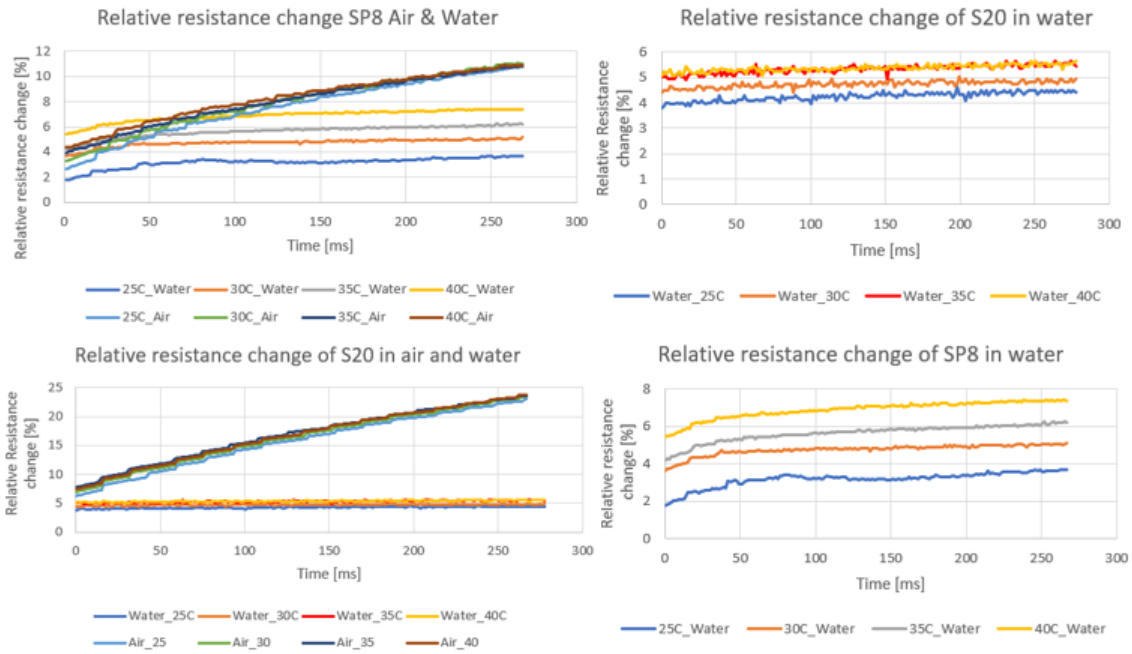

Figure 5-2 Overview of graphical results susceptibility tests

As noted in paragraph 4.2.8 and displayed in Figure *5-2* the values of the measuring sets changed due to external temperature influences. In the case of the relative resistance change of S20 in water, a more clear table can be found in Appendix 2. This influence was due to the fact that the relative resistance change was calculated in accordance with equation 4.11. In this case $R_{original}$ was the original resistance measured with 4 wire measurement at 20°C. However, if this is taken into account and the $R_{original}$ is replaced by a resistance value measured at the actual ambient temperature then influence of these ambient temperatures will be cancelled out in the calculations. It is therefore important to know what the ambient temperatures are during each measurement and to take them into account when calculating the relative resistance change.

Thermal image tests

The results of the thermal test can be found in paragraph 4.2.10 while the respective thermal images can be found in Table 5. The images displayed that the round shape of the printed heaters showed to provide a more homeogenous heating while the square shape of the microtechnical heaters had less heat in the corners resulting in heat being focust in the center of the sensor. Further coldspots were discovered in the printed heaters. It was proven by Dektak measurements that these slightly colder areas were the result of inconsistency in the printed conductive lines which were found in the form of varying heights in the ink. This inconsistency was the result of variations in distance and pressure between the screen and the sensor during screen printing.

Oven tests

The oven test showed that both heaters have a very similar thermal coefficient with that of the microtechnical heater being slightly higher. Considering the fact that the thermal coefficient of silver is normally slightly higher than that of gold $0{,}003819K^{-1}$ versus $0{,}003715K^{-1}$, sensors made with silver ink are in general a better choice for the envisioned measuring principle. However these values were lowered to $0{,}0016K^{-1}$ and $0{,}0014K^{-1}$ respectively due to influence of the thermal strain. This phenomenon is present when firmly attached films have a different thermal coefficient as their substrates leading the strain on the coefficient of resistivity for the bulk of the material to increase with increasing film thickness [25].

5.2.4 Conclusions for application of sensors

During this thesis 4 types of sensors were discussed: a printed capacitive moisture content sensor, a printed thermal moisture content sensor, a printed self-regulating moisture content sensor and a microtechnical thermal moisture content sensor.

From the perspective of building costs, the printed sensors have a clear advantage over their microtechnical counterparts. The building steps mentioned in paragraph 2.1.3 and 2.3.1 for the capacitive and thermal printed moisture sensors respectively are less labor intensive and require less man hours than those of the microtechnical heaters mentioned in 2.2.3.

A higher cost in production comes along with greater sensitivity as microtechnical heaters display a higher sensitivity than all other thermal sensors. As was discussed in paragraph 5.2.3 the main contributing factor was the fact that these sensors were thinner than their counterparts. This of course still leaves room from improvement of the printed heater. Bigger heaters showed to be more accurate while thinner heaters showed to be more susceptible to noise which makes size also an important factor in sensitivity.

Susceptibility to ambient influences is a major concern to all types of sensor applications as it influences the reliability of their measured results. In the case of the capacitive sensors, susceptibility to relative humidity changes was a concern due to the nature of its base design. An alteration consisting of adding a layer of T_iO_2 proved to diminish ambient influences to the

capacitive sensors. The thermal moisture content sensors were subjected to varying ambient temperatures to test their susceptibility as discussed in paragraph 4.2.8. It was found that they would need to take into account the external temperature in their calculations for relative resistance change. This would mean ambient temperatures should be known during the measurements by means of an external measurement.

A final factor in choosing an application for all these sensors is measurability and direct interpretation of the results. In the case of the capacitive sensor, the measurement signal is directly linear to the amount of moisture content. In this case, no more calculations or hardware is needed. In the case of the thermal moisture content sensors the measurement signal is current which is further recalculated to resistance and relative resistance change.

Concerning applications this would mean the sensors would divided in use cases were its either desirable to have a cheaper or more sensitive sensor. In the case were a cheaper sensor is desired, the capacitive sensor is the best option. This is due to it having few production steps requiring a low amount of man hours and it does not require any further data processing. This could be used in a cheap mass produced t-shirt for joggers for example were the amount of moisture should only be indicated and not accurately measured. In cases were accurate measurement is required the thermal heaters offer the best solution. Of these, the thinner microtechnical heater provided highest sensitivity. As it required the most production steps and labor to make, this sensor is more of interest in applications were need of greater sensitivity outweighs the concern of a higher price. This could for instance be for a characterization measurement performed by the company that produces the earlier mentioned t-shirts for joggers. The printed heaters could be a valuable and cheaper alternative to the microtechnical heaters if their sensitivity can increase enough by production of thinner sensors.

5.2.5 Outlook

Capacitive moisture content sensors

The effectiveness of the new added TiO_2 layer was not tested on the new setup due to a lack of time. As this setup is more reliable than the old setup, the benefit of the TiO_2 layer should be reestablished using this method. At the moment the amount of capacitance measured in farad is indicative of the amount of moisture that is present in the textile. A further expansion upon this work could be to find a way to measure the exact amount of moisture in the cloth. This can for instance be done by linking the relative permittivity of the moisture and the material in equations calculating the capacitance in general utilizing the permittivity of the material and taking into account the permittivity of water [26] [27] .

Printed thermal moisture content sensors

The printed thermal heaters could improve greatly in sensitivity from being thinner. Therefore options regarding printing on thinner Polyimide foils should receive a closer look. Another aspect that could be improved is the Polyimide tape which is needed to cover the printed heaters. The tape in question is 50µm thick and printed solutions such as a thin dielectric layer might help creating a thinner sensor. The entire printing process of the sensors can be optimized taking into account surface energy and ink. Inkjet printing instead of screen printing can also aid in reducing overall thickness of the sensors. Further it should be noted that both institutions have knowledge and options regarding inkjet printing which might provide an opportunity for cooperative research. Further the susceptibility tests pointed out that there is a need for external temperature monitoring or at least the need to take external temperatures in account when calculating measurement results. This means that it might be worth while looking into means to incorporate external temperature measurements in the overall measurements.

Printed self-regulating moisture content sensors

The self-regulating heaters performed similar to the regular printed heater in most cases ,however, after reaching 70 degrees the material starts behaving as a negative temperature coefficient material. Which means the sensor is currently not usable over this temperature as this would mean the two temperatures would have the same resistance value leading to uncertainty in the measurement. As was the displayed in

Figure 4-15, the self-regulating heaters sometimes performed different than anticipated. More research and data is required in order to make solid conclusions about their behavior and properly make use of their abilities.

Microtechnical heaters moisture content sensors

As discussed in paragraph 4.2.10 the microtechnical sensors had an inhomogeneous heat dissipation. This could be altered by adopting a round design. Another possible option might be experimenting with a microtechnical heater which has a lower resistance on the outside of its heater structure. Further the susceptibility tests pointed out that there is a need for external temperature monitoring or at least the need to take external temperatures in account when calculating measurement results. This means that as with the printed thermal moisture sensors it might be worth while looking into means to incorporate external temperature measurements in the overall measurements.

Appendices

Appendix 1A

Heater value's

Microtechnical heater			
Sensor	Oppervlak [mm²]	4Wire_R [Ω]	Voltage [V]
S1	/	423,7	/
S2	/	375	/
S3	/	351	/
S4	/	372	/
S5	/	406,75	/
S6	/	391,7	/
S7	/	400,6	/
S8	/	358,31	/
S9	/	385,6	/
S10	/	0	/
S11	/	371,15	/
S12	/	400	/
S13	/	386,9	/
S14	1	405,95	3,185710282
S15	/	391	/
S16	1	390,19	3,123259515
S17	25	395,47	15,72160138
S18R	25	385,45	15,52115492
S19	100	388,35	31,15886712
S20	100	363,34	30,13884537
S21	25	379,32	15,39724001
S19R	100	387,66	31,13117409
S14R	1	397,88	3,153886491

Printed regular heater				
Sensor	Thickness [µm]	Oppervlak [mm²]	R [Ω]	Voltage [V]
SP1	/	1661,902514	72,2	54,769828
SP2	50	153,93804	95,8	19,201083
SP3	/	254,4690049	nok	nok
SP4	/	1661,902514	68,9	53,503524
SP5	/	153,93804	90	18,610765
SP6	/	not ok	not ok	not ok
SP7	75	1661,902514	86,2	59,844799
SP8	75	153,93804	117,6	21,273877
SP9	/	254,4690049	67,3	20,691643
SP10	75	1661,902514	68,7	53,425814
SP11	75	153,93804	98,682	19,487761
SP12	75	254,4690049	49,6	17,76349
SP13	/	1661,902514	110,9	67,879487
SP14	/	254,4690049	21,2	11,613293
SP15	/	153,93804	49,8	13,843874
SP16	/	1661,902514	68,2	53,231042
SP17	50	254,4690049	42,7	16,481677
SP18	/	153,93804	80	17,546398
SP19	/	1661,902514	130	73,492742
SP20	75	254,4690049	85,4	23,308611
SP21	/	153,93804	177,8	26,15826

Surface area of printed heater			P_continuous	
A=3,14*r² [mm²]			25	mW/mm²
Small	r=7	153,938	0,025	W/mm²
Med	r=9	254,469		
Large	r=23	1661,903		

Self regulating heater				
Sensor	Thickness [µm]	R [Ω]	A [mm²]	U [V]
SS1	140	7,9	100	4,444097
SS2	75	20,7	100	7,193747
SS3	125	30	100	8,660254
SS4	140	61,03	100	12,35213

Thick foil				
Sensor	Thickness foil	R [Ω]	A [mm²]	U [V]
ST1		115,38	1	1,698382

Appendix 1 Overview of used heaters

Relative resistance change in water[%]																				
Time	**0**	**1,5**	**3**	**4,5**	**6**	**7,5**	**9**	**10,5**	**12**	**13,5**	**15**	**16,5**	**18**	**19,5**	**21**	**22,5**	**24**	**25,5**	**27**	**28,5**
Water_25C	3,799079	3,864083	4,00738	4,00738	3,942196	3,942196	3,942196	4,00738	3,942196	4,00738	3,942196	3,864083	4,00738	3,864083	4,072646	4,072646	4,00738	4,00738	4,072646	4,00738
Water_30C	4,413352	4,479128	4,479128	4,479128	4,676955	4,61093	4,544987	4,544987	4,479128	4,544987	4,544987	4,544987	4,479128	4,544987	4,479128	4,544987	4,676955	4,676955	4,61093	4,479128
Water_35C	5,021636	5,021636	5,021636	4,955175	4,955175	4,955175	4,955175	5,154811	5,154811	5,021636	5,021636	4,888798	5,088181	5,154811	5,154811	5,154811	5,154811	5,021636	5,088181	5,021636
Water_40C	5,088181	5,221525	5,154811	5,221525	5,301694	5,088181	5,088181	5,154811	5,221525	5,088181	5,154811	5,43558	5,301694	5,221525	5,154811	5,154811	5,221525	5,154811	5,301694	5,154811

Appendix 2 S20 microtechnical heater tested in water of different temperatures

Appendix 1B

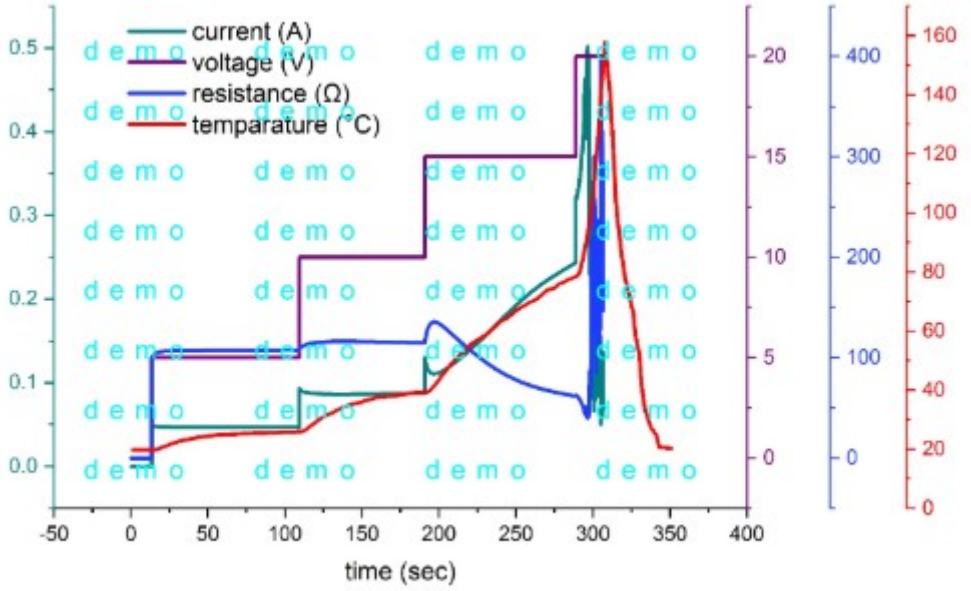

Appendix 3 Characterization of a self-regulating heater

Measurements and results can be found on added cd.

Bibliography

[1] https://www.hs-kl.de/informatik-und-mikrosystemtechnik/fachbereich/, "Fachbereich - Hochschule Kaiserslautern." [Online]. Available: https://www.hs-kl.de/informatik-und-mikrosystemtechnik/fachbereich/. [Accessed: 10-Feb-2018].

[2] UHasselt, "https://www.uhasselt.be/UH/IMO/About-IMO-IMOMEC." .

[3] D. Schönfisch, "Visual information provided by Fachhochschule Zweibrücken."

[4] T. Unander and H. E. Nilsson, "Characterization of printed moisture sensors in packaging surveillance applications," *IEEE Sens. J.*, vol. 9, no. 8, pp. 922–928, 2009.

[5] T. Unander, *Characterization of Low Cost Printed Sensors for Smart Packaging*. 2008.

[6] J. Y. , Jia, K. , Sun, M., "A resonant printed-circuit sensor for remote query monitoring of environmental parameters."

[7] F. Jin, H. Tong, L. Shen, K. Wang, and P. K. Chu, "Micro-structural and dielectric properties of porous TiO 2 films synthesized on titanium alloys by micro-arc discharge oxidization," *Mater. Chem. Phys.*, vol. 100, pp. 31–33, 2006.

[8] N. Suppression, L. Filters, and T. Effect, "Characteristic of Capacitors The Effect of Non ideal Capacitors," pp. 12–14.

[9] I. Parkova, I. Ziemele, and A. Vi, "Fabric Selection for Textile Moisture Sensor Design," pp. 1–3, 2012.

[10] D. Schönfisch, "PhD Progress Report 2017."

[11] S. Tobias, *Publicly disclosed bachelor's thesis provided by Fachhochschule Zweibrücken*. 2018.

[12] "Elegoo Klebeband 3D Drucker Hitzebeständiges Tape Polyimid Elektronik Isolierband 33M Bandlänge: Amazon.de: Gewerbe, Industrie & Wissenschaft." [Online]. Available: https://www.amazon.de/Hitzebeständiges-Klebeband-Elektronik-Isolierband-Bandlänge/dp/B0732ZSS5V/ref=sr_1_1?ie=UTF8&qid=1523262210&sr=8-1&keywords=kapton+tape. [Accessed: 22-May-2018].

[13] "LC meter – LC100x User Guide – ElecFreaks – Devote to open hardware." [Online]. Available: https://www.elecfreaks.com/1597.html. [Accessed: 06-Mar-2018].

[14] Rev, "LC100-A Digital L/C Meter Inductance Capacitance Meter User Manual."

[15] "LC100A Digital LC Meter Inductor Capacitor Inductance Capacitance CAP Tester | eBay." [Online]. Available: http://www.ebay.com.au/itm/LC100A-Digital-LC-Meter-Inductor-Capacitor-Inductance-Capacitance-CAP-Tester-/231371116034. [Accessed: 05-Mar-2018].

[16] "A Guide to Resistance Measurement - Seaward." [Online]. Available: http://www.seaward.co.uk/resistance-measurement. [Accessed: 27-May-2018].

[17] "Datasheet SHT3x-DIS Benefits of Sensirion's CMOSens ® Technology."

[18] "How an n-Channel MOSFET works." [Online]. Available: http://macao.communications.museum/eng/exhibition/secondfloor/MoreInfo/2_10_4_HowFETWorks.html. [Accessed: 20-Mar-2018].

[19] "Specific Heat of common Substances." [Online]. Available: https://www.engineeringtoolbox.com/specific-heat-capacity-d_391.html. [Accessed: 28-May-2018].

[20] "What Is Thermal Effusivity? What's The Difference From Thermal Conductivity?" [Online]. Available: http://www.acttr.com/en/en-faq/en-faq-thermal-analysis/298-en-faq-what-is-

thermal-effusivity.html. [Accessed: 28-May-2018].

[21] DuPont, “DuPont Kapton HN Technical Data Sheet,” 2011.

[22] “C2131014D3 Flexible Silver Paste Gwent Group,” p. 2131014.

[23] “Temperature Coefficient of Resistance | Physics Of Conductors And Insulators | Electronics Textbook.” [Online]. Available: https://www.allaboutcircuits.com/textbook/direct-current/chpt-12/temperature-coefficient-resistance/. [Accessed: 11-May-2018].

[24] F. Warkusz, “The size effect and the temperature coefficient of total resistance in thin metal films,” *J. Phys. D. Appl. Phys.*, vol. 11, no. 14, pp. 2035–2041, Oct. 1978.

[25] F. Warkusz, “The size effect and the temperature coefficient of resistance in thin films,” *J. Phys. D. Appl. Phys.*, vol. 11, no. 5, pp. 689–694, 2001.

[26] Ajayan K R and K. J. Vinoy, “Planar Inter Digital Capacitors on Printed Circuit Board.”

[27] R. Igreja and C. J. Dias, “Extension to the analytical model of the interdigital electrodes capacitance for a multi-layered structure,” *Sensors Actuators, A Phys.*, vol. 172, no. 2, pp. 392–399, 2011.

Auteursrechtelijke overeenkomst

Ik/wij verlenen het wereldwijde auteursrecht voor de ingediende eindverhandeling:
Evaluation and comparison of printed and microtechnically fabricated moisture sensors for textile applications

Richting: **master in de industriële wetenschappen: energie-automatisering**
Jaar: **2018**

in alle mogelijke mediaformaten, - bestaande en in de toekomst te ontwikkelen - , aan de Universiteit Hasselt.

Niet tegenstaand deze toekenning van het auteursrecht aan de Universiteit Hasselt behoud ik als auteur het recht om de eindverhandeling, - in zijn geheel of gedeeltelijk -, vrij te reproduceren, (her)publiceren of distribueren zonder de toelating te moeten verkrijgen van de Universiteit Hasselt.

Ik bevestig dat de eindverhandeling mijn origineel werk is, en dat ik het recht heb om de rechten te verlenen die in deze overeenkomst worden beschreven. Ik verklaar tevens dat de eindverhandeling, naar mijn weten, het auteursrecht van anderen niet overtreedt.

Ik verklaar tevens dat ik voor het materiaal in de eindverhandeling dat beschermd wordt door het auteursrecht, de nodige toelatingen heb verkregen zodat ik deze ook aan de Universiteit Hasselt kan overdragen en dat dit duidelijk in de tekst en inhoud van de eindverhandeling werd genotificeerd.

Universiteit Hasselt zal mij als auteur(s) van de eindverhandeling identificeren en zal geen wijzigingen aanbrengen aan de eindverhandeling, uitgezonderd deze toegelaten door deze overeenkomst.

Voor akkoord,

Booten, Matthias

Datum: **4/06/2018**